Supplementary Information (SI) for RSC Advances.
This journal is © The Royal Society of Chemistry 2024

Communicated to: *RSC Adv.*,
Ms. Type: *Article*
Ms. No.: RA-ART-04-2024-002584-R2

Supplementary Materials

Mixed-ligand copper(II)-diimine complexes of 3-formylchromone-N^4-phenyl thiosemicarbazone: 5,6-dmp co-ligand confers enhanced cytotoxicity

Anjaneyulu Mamindla,[a] Dhanashree Murugan,[b] Manikandan Varadhan,[a] Tamilarasan Ajaykamal,[c] Loganathan Rangasamy,[b] Mallayan Palaniandavar*[c] and Venugopal Rajendiran*[a]

[a]*Department of Chemistry, School of Basic and Applied Sciences, Central University of Tamil Nadu, Thiruvarur 610005, India. E-mail: rajendiran@cutn.ac.in*

[b]*Drug Discovery Unit (DDU), Centre for Biomaterials, Cellular and Molecular Theranostics (CBCMT), Vellore Institute of Technology (VIT), Vellore 632014, Tamil Nadu, India*

[c]*School of Chemistry, Bharathidasan University, Tiruchirappalli 620024, India*

*****Corresponding authors.
Eamil adresses: rajendiran@cutn.ac.in (V. Rajendiran).

Materials

All reagents and chemicals were of analytical grade, obtained from different commercial sources, and used as received without any further purification unless and otherwise stated. 3-formyl chromone, 4-phenylthiosemicarbazide, 2,2'-bipyridine (bpy), 1,10-phenanthroline (phen), 5,6-dimethyl-1,10-phenanthroline (5,6-dmp), ethidium bromide (EthBr), agarose (molecular biology grade), superoxide dismutase (SOD), catalase (stored at -20 °C) and calf thymus (CT) DNA (highly polymerized; stored at 4 °C) were procured from Sigma-Aldrich (MO, USA). Human serum albumin and pUC19 supercoiled DNA (cesium chloride purified) were obtained from Bangalore Genei (India). For all buffer preparations and biological experiments, ultra-pure water (18.2 μΩ) was used. In DNA and protein binding experiments, <1% DMF/5 mM Tris HCl/50 mM NaCl buffer at pH 7.1 (Tris-HCl buffer) and phosphate buffer at pH 7.1, respectively, were used. Pyrazino[2,3-f][1,10]phenanthroline (dpq) ligand was prepared according to an already reported synthetic procedure.[1]

Physical measurements and experimental procedures

UV-visible absorption spectra and stability studies of all complexes were recorded on UV-2450 Shimadzu (Japan) spectrophotometer. Solid infrared spectra of the complexes were obtained using Shimadzu (Japan) FTIR working at a resolution of 2 cm^{-1} from 4000 to 400 cm^{-1}. A pre-calibrated digital conductivity meter was used to measure the molar conductivity (Systronics, India). The Avance NEO 400 MHz FT-NMR spectrometer was used to acquire the ^{1}H and ^{13}C NMR characterization. HR-MS data were recorded on a Thermo Fisher's (MA, USA) Q-Exactive plus-Quadrupole-orbitrap mass spectrometer. At the FLASH EA 1112 sequence, a CHN (O) analyzer from Thermo Finnigan was used to determine an elemental analysis of the complexes. Electron paramagnetic resonance spectra of the copper(II) complexes were obtained on a JEOL Model JES FA200 EPR spectrometer in DMF at liquid nitrogen temperature (LNT). Thermogravimetric analysis (TGA) was carried out from RT to 700 °C at a heating rate of 20 °C/min under N_2 atmosphere on a PerkinElmer-STA8000 simultaneous thermal analyzer. Utilizing a fluorescence spectrophotometer (Agilent Technologies 9800A Cary Eclipse, CA, USA), the DNA binding investigation was studied. A thermostatic water bath kept at a constant temperature of 20 °C was used to establish an Ubbelodhe viscometer (Cannon, PA, USA) to measure the viscosity of DNA solution. The DNA cleavage was quantified using ImageJ, which was used to calculate the percentage of

cleavage after the gel image was captured with a CCD camera (Vilber Lourmat gel documentation system, France, Alpha InfoTech Corporation). For cytotoxicity studies, the absorbance was measured using a microplate reader (Bio-rad iMark Microplate reader, USA) at 595 nm, and AO/EB-Hoechst 33258 assay cells were viewed under the fluorescent microscope (EVOS M5000 Imaging Systems, Thermo Fisher Scientific, USA) fitted with a DAPI Filter 395− 425 nm filter and observed at × 40 magnification.

Cyclic voltammetry

The electrochemical properties of the complexes have been examined using Cyclic voltammetry (CV) and differential pulse voltammetry (DPV) on a CH instrument (TX, USA), potentiostat at 25.0 ± 0.2 °C. A three-electrode system comprising of glassy carbon (3 mm), a platinum wire as an auxiliary electrode, and a reference electrode calomel was used. The experiment was performed in DMF with 0.1 M $[NBu_4]ClO_4$ supporting electrolyte.The solution was deaerated with pure N_2 for 15 minutes prior to each experiment, and a nitrogen atmosphere was maintained over the solution throughout each experiment. The anodic (E_{pa}) and cathodic (E_{pc}) peak potentials of the CV traces were used to determine the redox potential $E_{1/2}$ as $(E_{pa} + E_{pc})/2$. As an internal standard, the ferrocene (Fc^+/Fc) system was used. In DPV, the $E_{1/2}$ value was calculated by substituting the peak potential (Ep), which is obtained from the differential pulse voltammogram in this equation: $E_p + \Delta E/2$ (ΔE is the pulse height).[2]

Cell viability assay

Cytotoxicity of the synthesized free ligand and complexes **1**-**4** was evaluated through MTT assay in HeLa cell lines.[3–5] The cells (5×10^3 cells/well in 200 µL of media) were seeded onto 96 well plate and were allowed to grow for 24 h at 37°C, 5% CO_2. Cells were treated with increasing concentrations of compounds for 24 h and 48 h. The study was conducted in triplicates. DMSO and media were used as a negative control, and cisplatin was used as a standard drug, respectively. After 24 h and 48 h, 20 µl of MTT reagent (5 mg/ml in sterile distilled water) was added to each well, and plates were wrapped with aluminium foil and incubated for 4 h at 37 °C. The purple formazan product was dissolved by the addition of 100 µL DMSO to each well. The absorbance was measured using a microplate reader (Bio-rad iMark Microplate reader, USA) at 595 nm. Data were collected for three replicates each and

used to calculate the mean. The percentage inhibition was calculated from this data using the formula;

$$= \frac{\text{mean OD of untreated cells (control)} - \text{mean OD of treated cells}}{\text{mean OD of untreated cells (control)}} \times 100$$

IC_{50} values were calculated using dose-response inhibition curves in Graph pad prism.

AO/EthBr staining assay

HeLa cells (5.0×10^4/mL) were seeded in 24 well plate for 24 h. Based on the IC_{50} values of the compounds, complexes **2**, **3**, and **4** were selected for further analysis. 5 µM concentration of complexes and 20 µM concentration of cisplatin were added in each well and incubated for 24 h and 48 h, respectively. The culture suspensions were centrifuged to collect dead cells into an Eppendorf tube and, re-suspended in the PBS, and added to the respective wells. Acridine orange (100 µg/mL) and ethidium bromide (100 µg/mL) were prepared and mixed in a 1:1 ratio. 50 µl of AO/EB dye mixture was mixed into each well, and cells were viewed under the fluorescent microscope (EVOS M5000 Imaging Systems, Thermo Fisher Scientific, USA) fitted with a DAPI Filter 395− 425 nm filter and observed at × 40 magnification. Tests were done in triplicate.[3–5]

Hoechst 33258 staining assay

Cell pathology of compound-treated HeLa cells (5.0×10^4/mL) was detected by Hoechst 33258 (100 µg/mL) staining. [6] Based on the IC_{50} values of the compounds, complexes **2**, **3**, and **4** were selected for further analysis. 5 µM concentration of compounds and 20 µM concentration of cisplatin were added in each well and incubated for 24 h and 48 h, respectively. Suspended dead cells were centrifuged and re-suspended in 100 µl of PBS and were added to the respective well. These wells were subjected to 25 µl of Hoechst 33258 dye. At random, 100 cells were observed in a fluorescent microscope (EVOS M5000 Imaging Systems, Thermo Fisher Scientific, USA) fitted with a DAPI Filter 395− 425 nm filter and observed at × 40 magnification, and the percentage of cells reflecting pathological changes were calculated. Data were collected for triplicates and used to calculate the mean and the standard deviation.

Measurement of lipophilicity

The partition coefficients (*P*) of complexes **1-4** between octanol and water were determined using the shake-flask method.[7] To allow for phase saturation, n-octanol and Tris-HCl buffer were shaken for 24 hours. The stock solutions of each complex (1 mmol) were prepared in the aqueous phase, and aliquots (1 mL) of each of the four complex solutions were added to an equivalent volume of the n-octanol. The complex concentrations in the organic and aqueous phases were then determined using UV absorbance spectroscopy. Log *P* is the logarithm of the ratio of the concentrations of the tested complex in the organic and aqueous phases.

Cell culture

The National Centre for Cell Science (NCCS), Pune, India, provided the HeLa cervical cancer cell. The cells were grown at 37°C in a CO_2 incubator in DMEM in 24 well plates containing 10 % FBS (Hi-Media) (1 mL/well), 100 U/mL penicillin, and 100 g/mL streptomycin as antibiotics (Himedia, Mumbai, India) (Heraeus, Hanau, Germany). Cells were grown in 96-well plates for 24 or 48 hours for the experimental assays. The control drug cisplatin was purchased from Getwell Pharmaceuticals, Kochi, India. Cells from passage 15 or less were used in all of the experiments.[5,8,9]

In vitro DNA binding and cleavage experiments

All of the metal complexes are soluble in 10% DMF/5 mM Tris-HCl/50 mM NaCl buffer at pH 7.1 (10% DMF-Tris-HCl buffer), although they are all only partially soluble in water. Therefore, concentrated stock solutions of metal complexes were prepared by dissolving them in 10% DMF-Tris-HCl buffer and dilution with the solution to perform DNA binding and cleavage studies, appropriate buffer for each experiment. According to the previously published process, CT-DNA stock solution preparation and concentration determination were accomplished.[10]

EthBr displacement assay

Typically, 125 μM of CT-DNA solution is added to a 2 mL solution of EthBr in a binding experiment was included to clarify the EthBr's maximum fluorescence intensity (excitation at 450 nm; emission range 500–600 nanometers) in 10% DMF–Tris–HCl buffer.

Subsequently, 10 μM aliquots of solutions of the complexes **1-4**, in 10% DMF-Tris-HCl buffer, were added to the EthBr-bound CT-DNA solution. Following that, the emission, depending the extent to which metal complexes could break the EthBr-DNA binding, intensity decreased. The plot of these given function for the determination of the apparent DNA-binding constant (K_{app}) values. intensities against complex concentrations, using the equation

$$K_{EtBr}[EthBr] = K_{app}[complex] \quad (1)$$

Where K_{EthBr} is 4.94 x 10^5 M^{-1}, the concentration of EthBr is 12.5 μM, and the concentration of the complex is that used to obtain a 50% reduction of fluorescence intensity of EthBr" .[11]

Viscosity experiments

The Ubbelodhe viscometer was used to monitor the change in DNA viscosity while keeping a constant temperature of 20 °C in order to determine the nature of the molecular interaction of the complexes with the CT-DNA. When adding the complex **1-4**, the viscosity of the 10% DMF-Tris-HCl buffer containing the stock solution of DNA was evaluated after each addition of the complex at concentrations ranging from (1/R 0 to 0.5) to 200 μM CT-DNA. Prior to each addition, the mixture was allowed to reach equilibrium for 5 minutes. The results was then plotted as "$(\eta/\eta_0)^{1/3}$ versus 1/R, where η and η_0 represent the viscosity of DNA in the presence of the complex and the viscosity of DNA alone in buffer solution, respectively" [9].

Protein binding study

Tryptophan fluorescence quenching studies were used to evaluate the protein binding using human serum albumin (HSA, 5 μM) as the substrate in phosphate buffer (pH 7.1) and the copper complexes **1-4** as quenchers (Q). The intensity of the tryptophan residue's (Trp214) emission was seen at 347 nm as the quencher was gradually added to the HSA solution (excitation wavelength at 295 nm).[12,13] Fluorescence measurements were performed using a 1 cm quartz cell on a Fluorescence Spectrophotometer (Agilent Technologies). Similar experimental setups were used to record the emission spectra of the complexes, and no emission band in this region was observed. "Stern-Volmer equation [14] and plots I/I_0 vs [complex] were employed to calculate the dynamic quenching constant K_{SV} (in M^{-1}) for the interaction of each quencher with HSA".

DNA cleavage studies

Using agarose gel electrophoresis, the cleavage of complexes **1 -4** with supercoiled pUC19 DNA were observed. Copper complexes made in the same 10% DMF-Tris-HCl

solution were used to treat the plasmid DNA (SC form, 40 μM). In this experiment, the pUC19 plasmid DNA (SC form, 40 μM) in Tris-HCl buffer was treated with 100 μM copper complexes in the absence and presence of ascorbic acid (H_2A, 50 μM), respectively. The reaction mixtures were then incubated at 37°C for 4 h in the absence of the H_2A and 30 min in the presence of H_2A. Then, a loading buffer was added to the resulting mixture, and electrophoresis was conducted at 50 V for 4 h using 1% agarose gel containing 1.0 μg mL^{-1} EthBr in Tris-Acetate-EDTA (TAE) buffer containing 40 mM Tris base, 20 mM acetic acid, and 1 mM EDTA. The gels were viewed in a Gel Documentation System (Vilber Lourmat, France) and photographed using a CCD camera (Alpha InfoTech Corp). The plasmid DNA with a lower intensity was due to the lesser ability to bind ethidium bromide, compensated by a factor of 1.47.[15] The plasmid DNA cleavage efficiency was measured by densitometric calculation using ImageJ software, which determines the ability of the complexes to convert supercoiled DNA form (I) to nicked circular form (II) and linear form (III). Mechanistic studies were carried out by incubating the SC DNA and the complex in the presence of various scavengers, such as DMSO, sodium azide (NaN3), catalase, and SOD, to scavenge hydroxyl radical, singlet oxygen, H2O2, and superoxide, respectively. After the incubation, the gel was electrophoresed and examined, as previously mentioned.

Molecular docking simulation

Docking analysis was performed using the *AutoDock4* tool (an open-source software) to identify the intermolecular interactions and possible binding sites of the copper(II) complexes on DNA and HSA protein. The crystal structures of the B-DNA dodecamer d(CGCGAATTCGCG)2 (PDB id: 1BNA), (https://www.rcsb.org/structure/1bna) and HSA (PDB id: 8H0O) were obtained from the protein data bank (*https://www.rcsb.org/structure/8H0O*). The complexes' 3D SDF mol file structure was generated from the 3D Chemdraw software, and the drawn structures were optimized using Avogadro software and saved as SDF mol files. Then, these SDF files were then converted to the PDBQT format using the OPENBABEL (http://www.vcclab.org/lab/babel/) software. The obtained data was visualized with the help of the Discovery Studio molecular graphics and protein-ligand interaction profiler (PLIP). By using this software, 3D conformations of protein-complex interaction profiles of hydrogen-bonding interactions (*H*-B), electrostatic interactions

(ES), and van der Waals (vdW) interactions were generated. The best binding complex was selected based on binding energy and is calculated using an equation.[16]

$$\Delta Ebinding\ energy = \Delta E_{vdw} + \Delta E_{H\text{-B}} + \Delta E_{\text{ES}}$$

Herein, ΔE_{vdw} = van der Waal energy, $\Delta E_{H\text{-B}}$ = hydrogen bonding energy, and ΔE_{ES} stands for electro statistic energy.

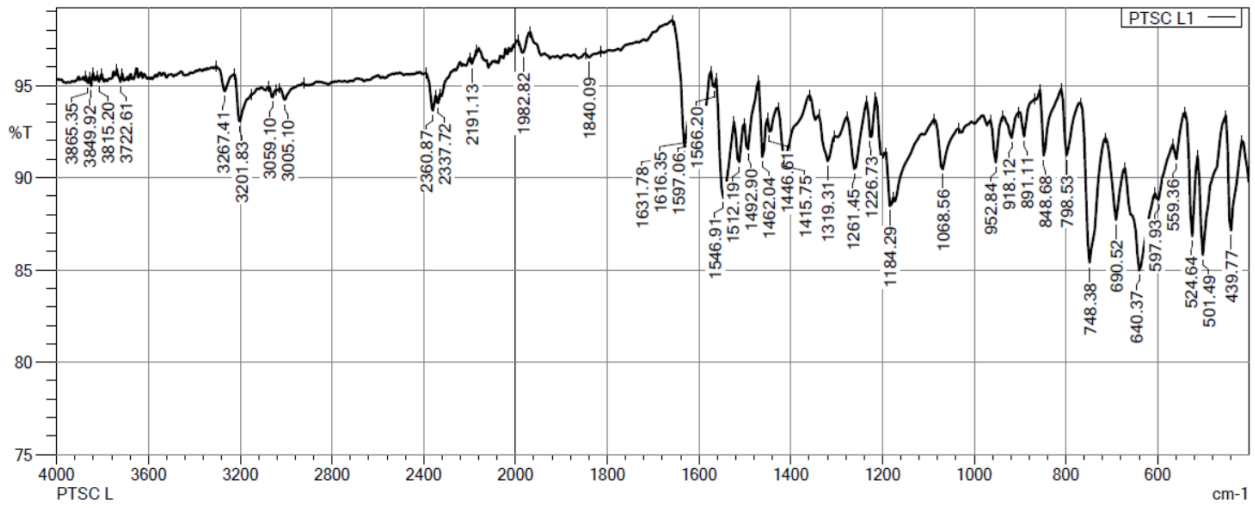

Fig S1. FT-IR spectrum of Ligand HL.

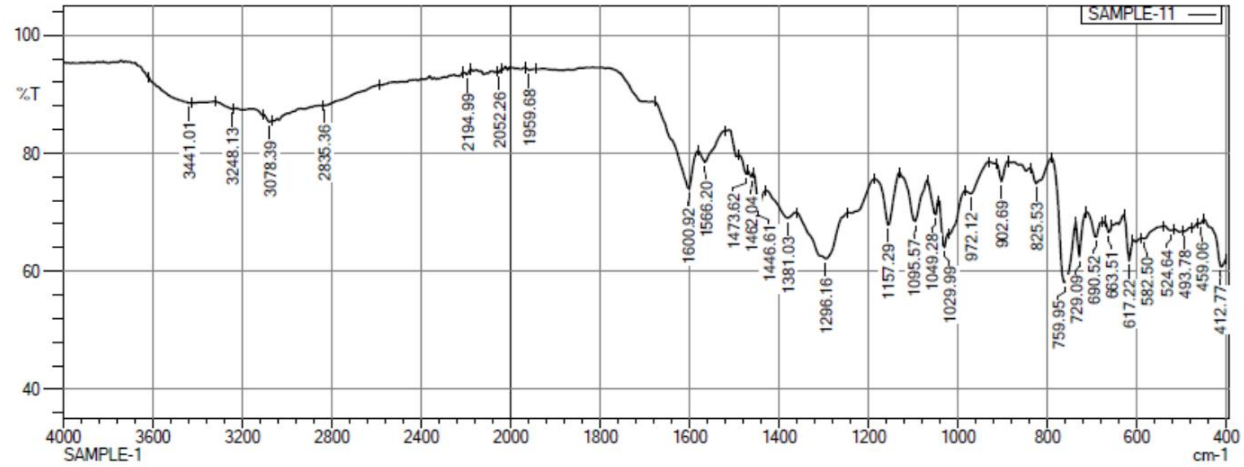

Fig S2. FT-IR spectrum of Complex **1**

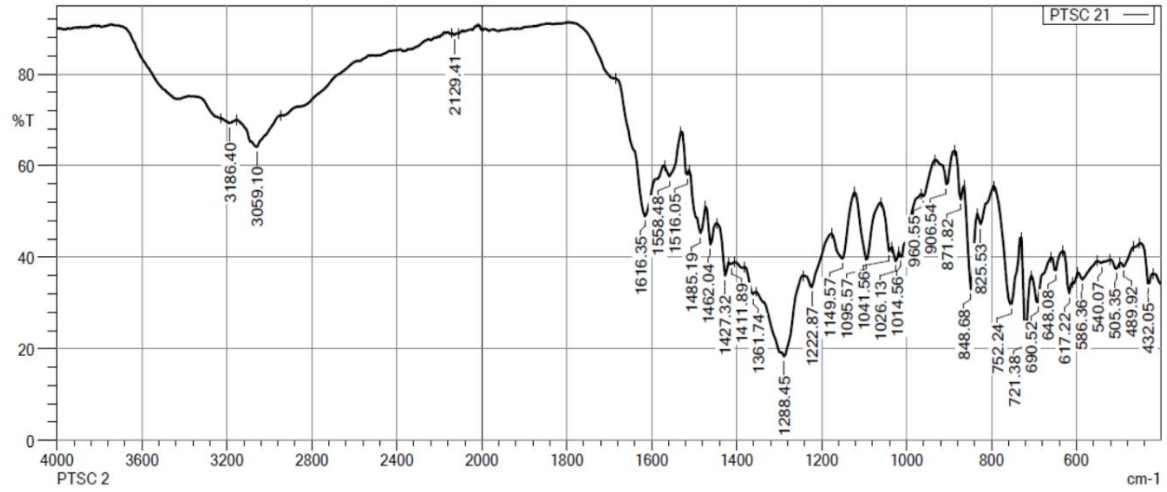

Fig S3. FT-IR spectrum of Complex **2**

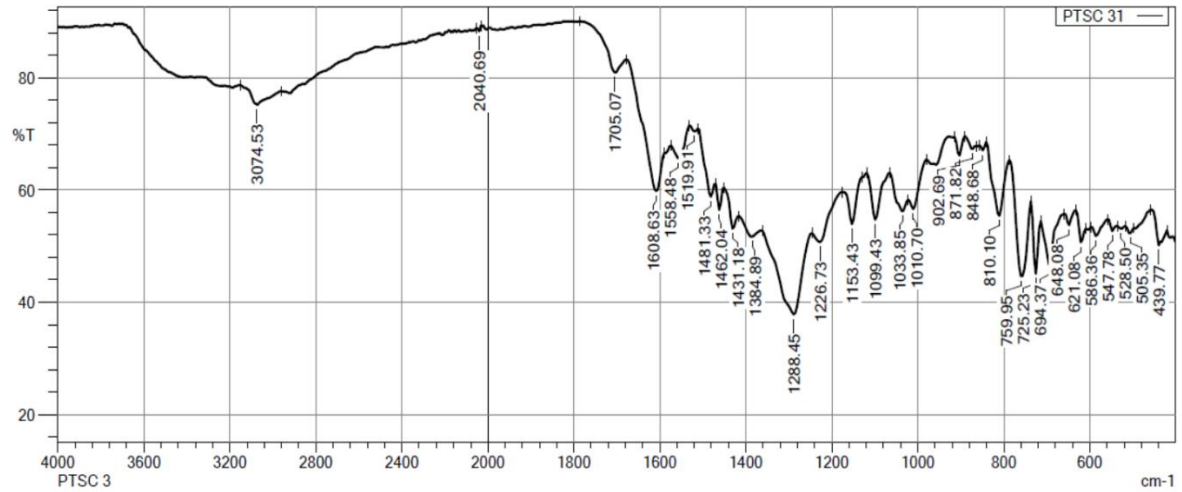

Fig S4. FT-IR spectrum of Complex **3**

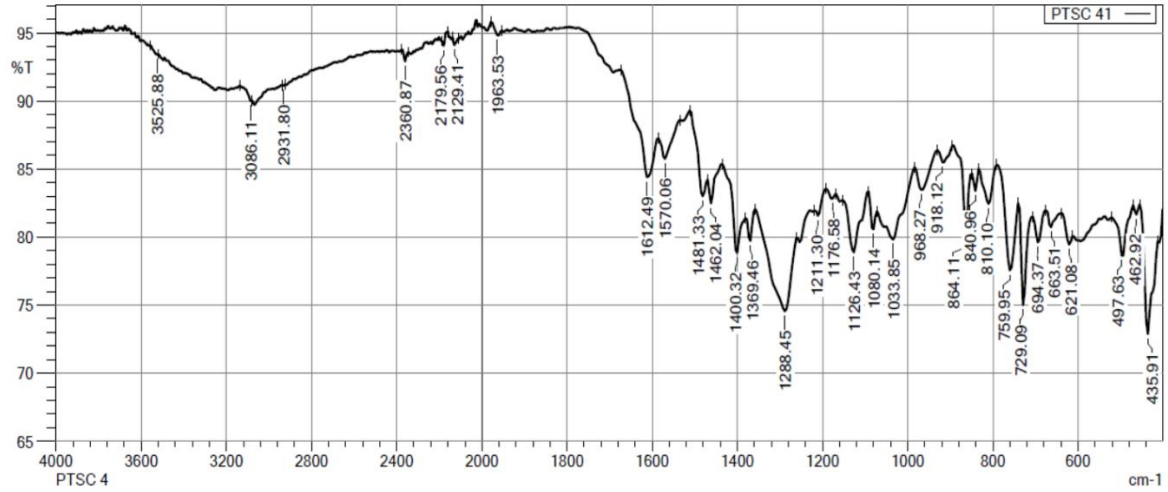

Fig S5. FT-IR spectrum of Complex **4**

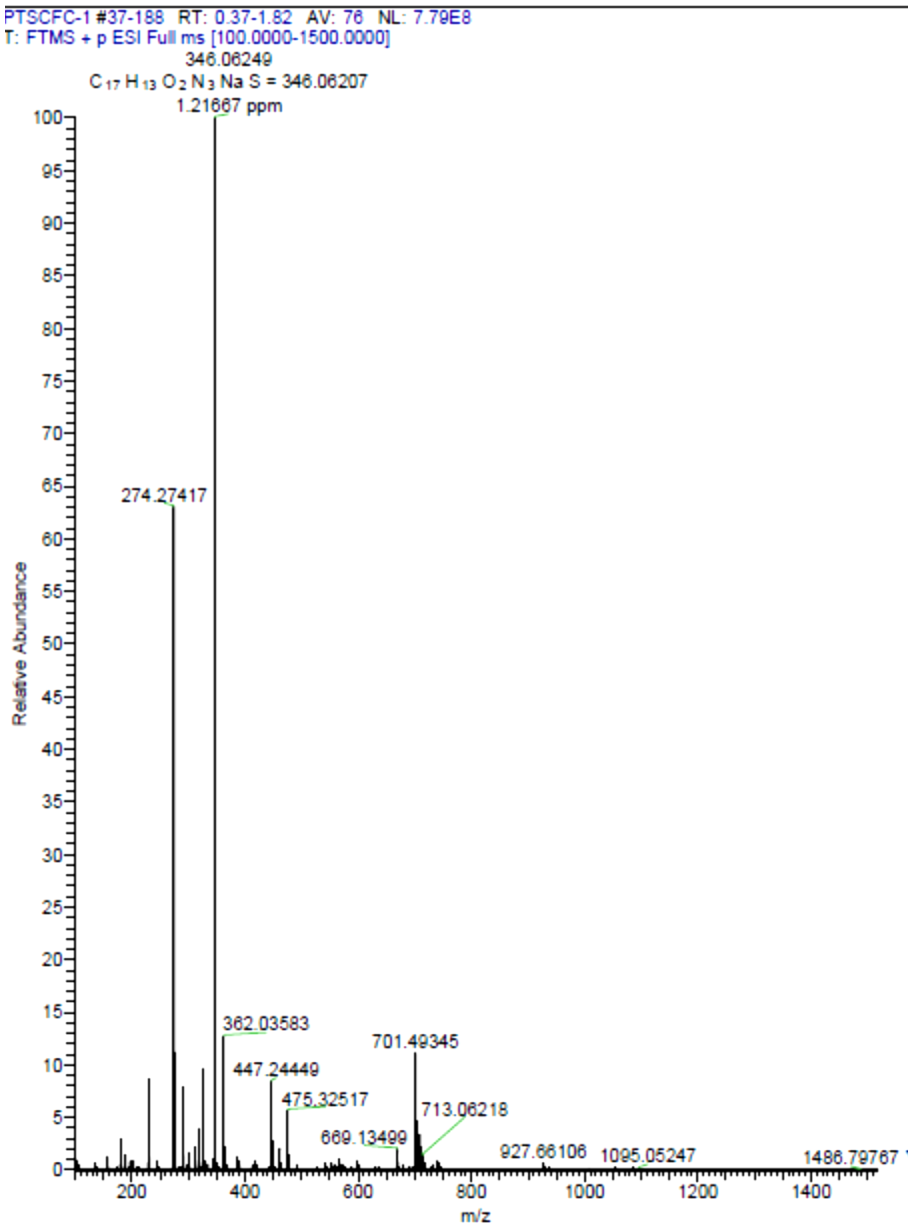

Fig. S6. Mass spectrum of ligand (HL) in methanol

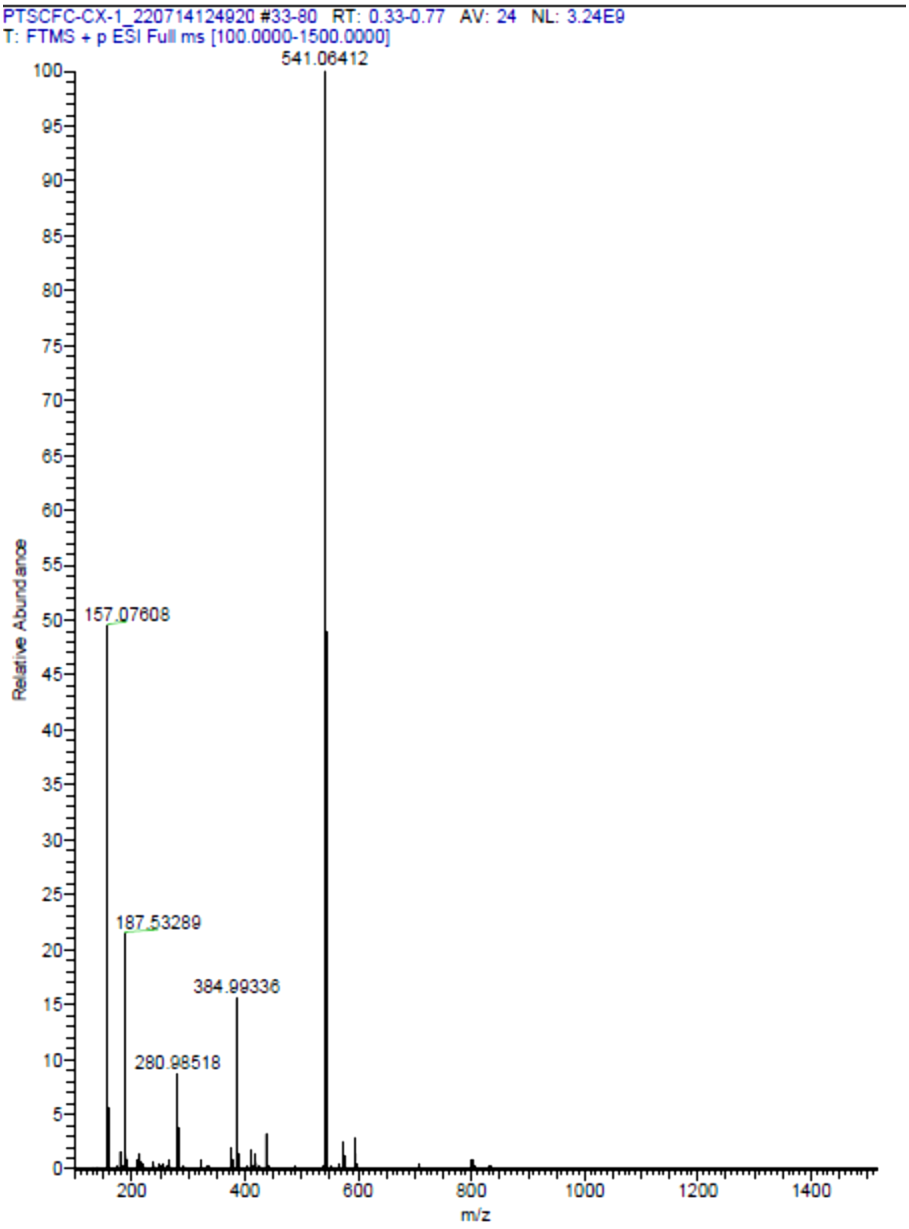

Fig. S7. Mass spectrum of Complex **1** in methanol

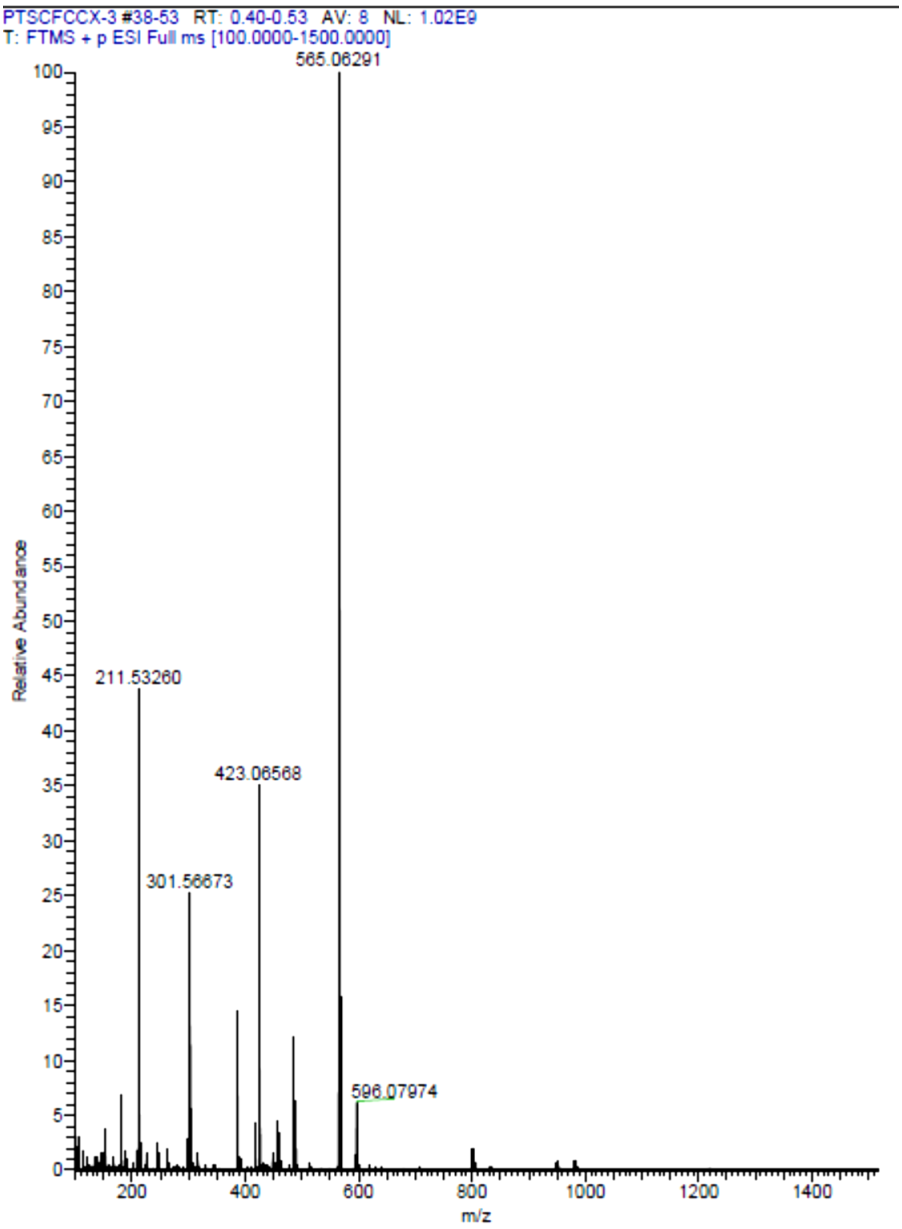

Fig. S8. Mass spectrum of Complex **2** in methanol

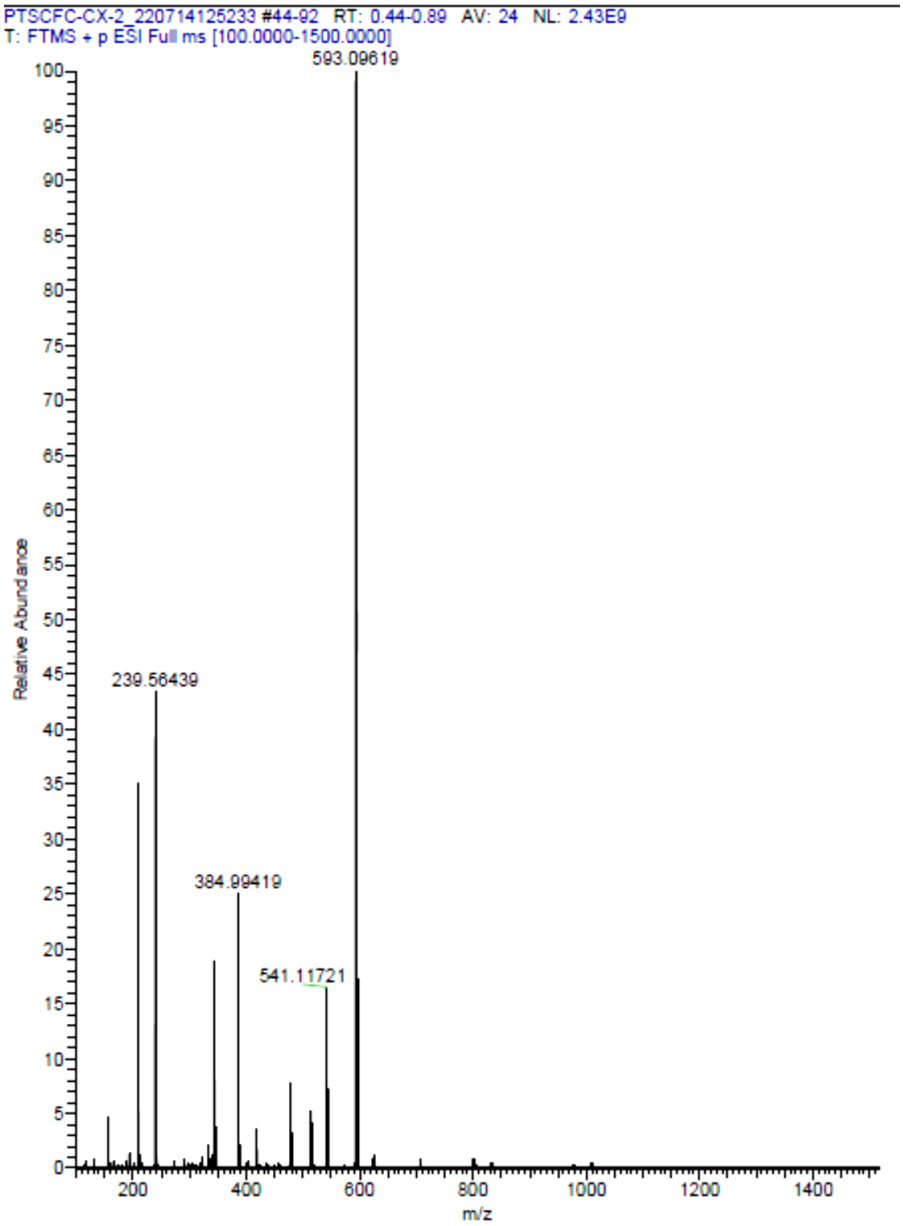

Fig. S9. Mass spectrum of Complex **3** in methanol

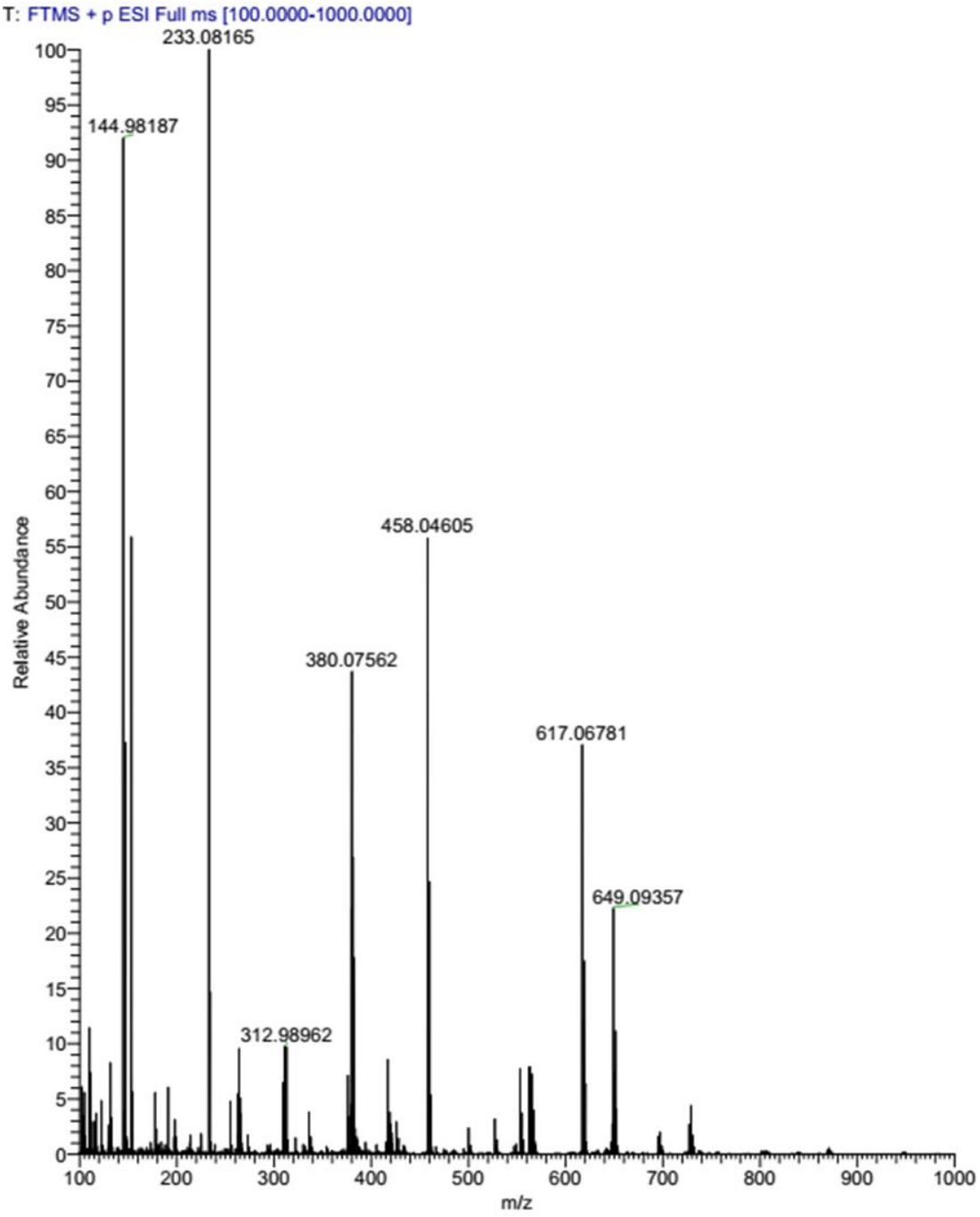

Fig. S10. Mass spectrum of Complex **4** in methanol.

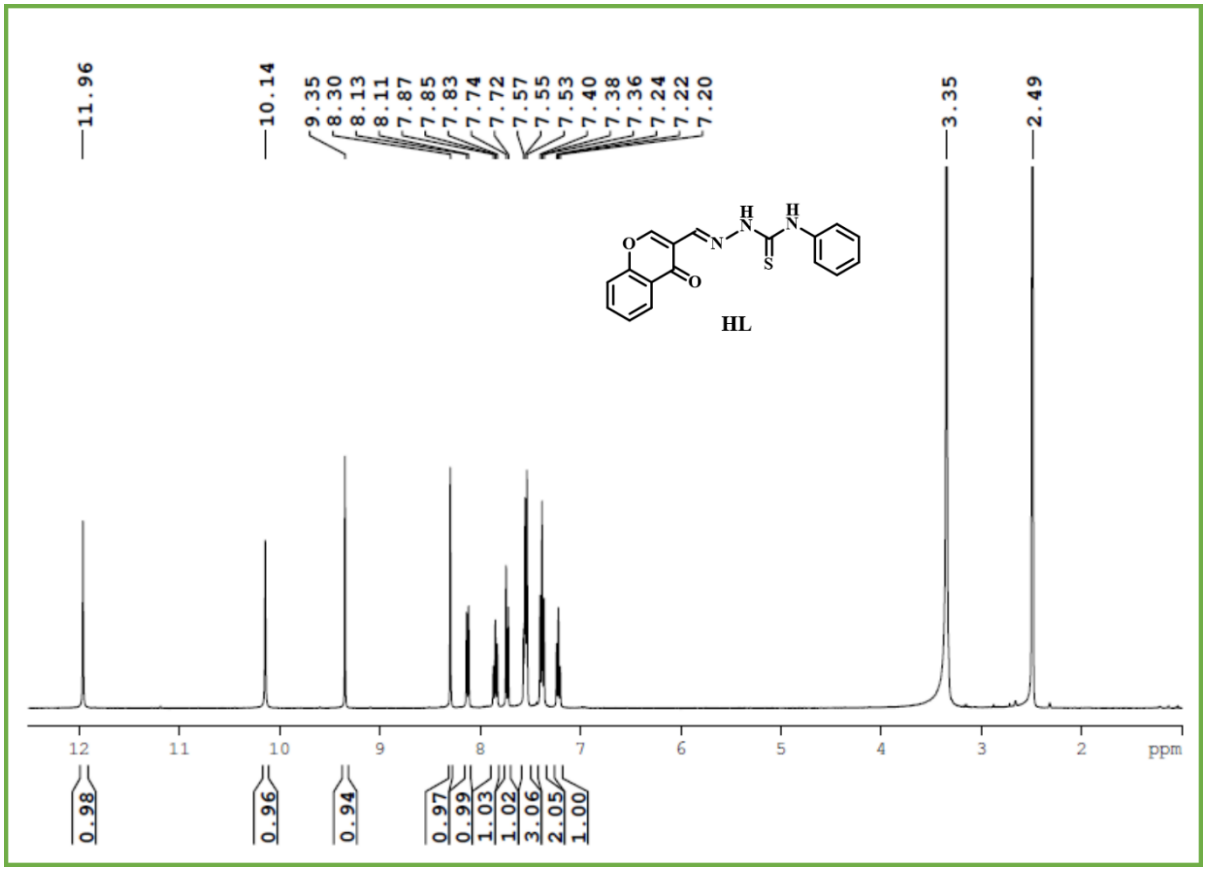

Fig. S11. ^{1}H-NMR spectrum of ligand (HL) in DMSO-d_6.

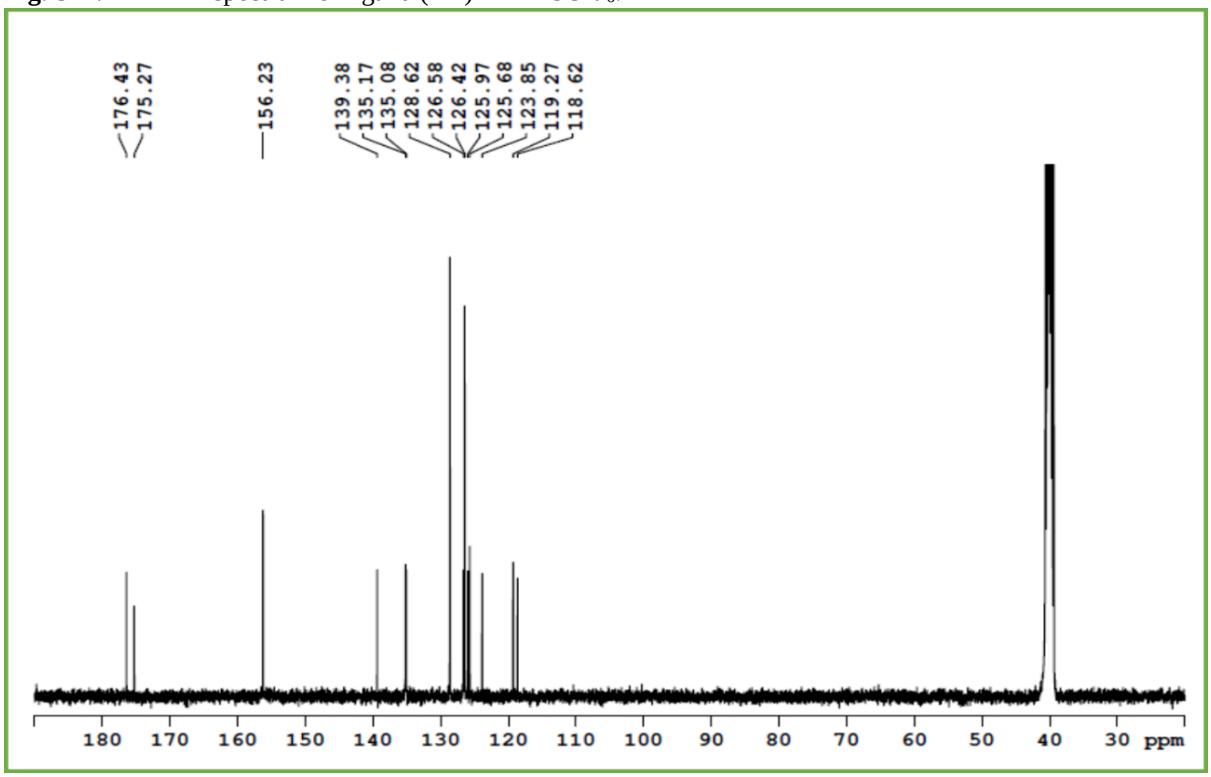

Fig. S12. ^{13}C-NMR spectrum of ligand (HL) in DMSO-d_6.

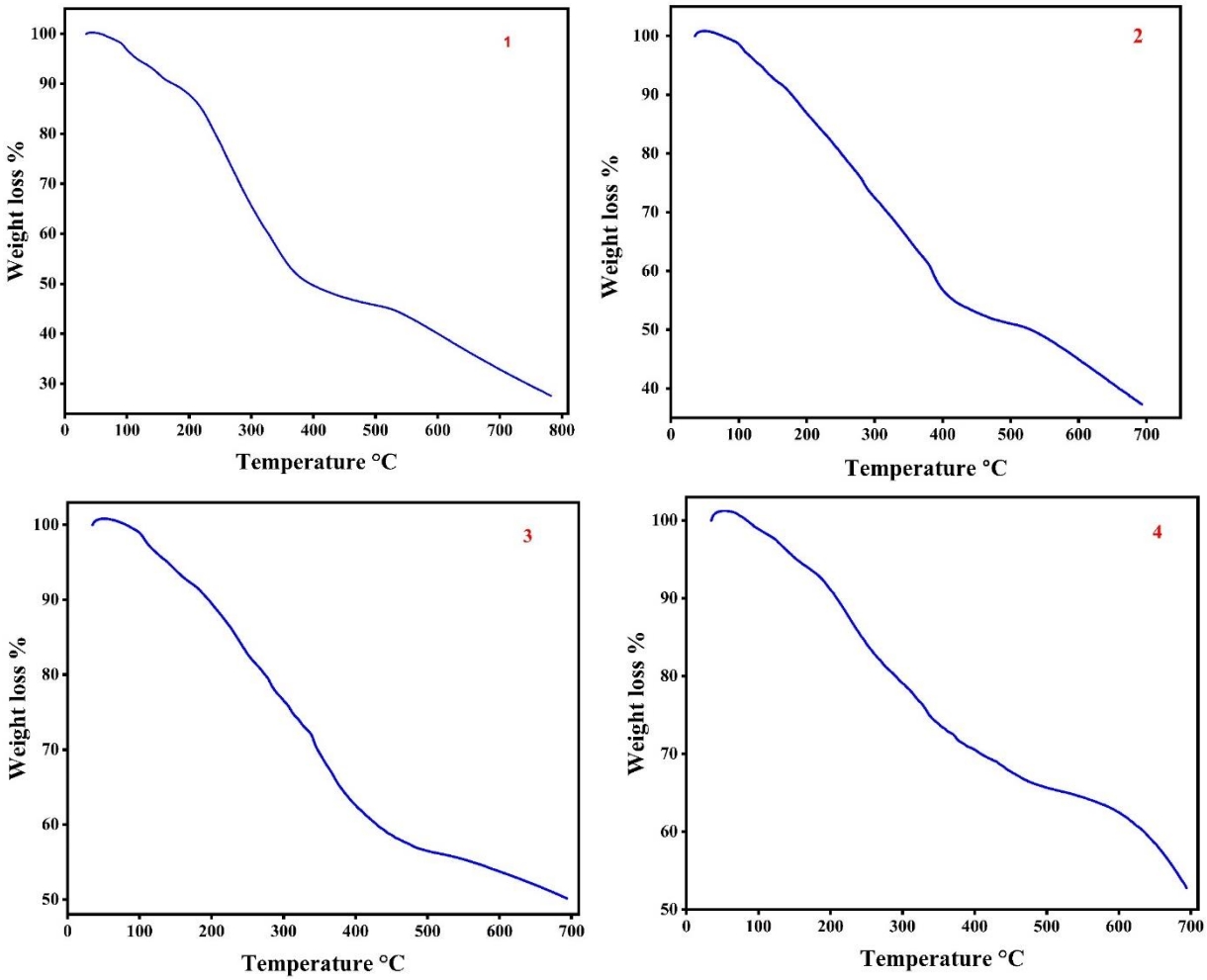

Fig. S13. Thermograms of complexes **1-4**.

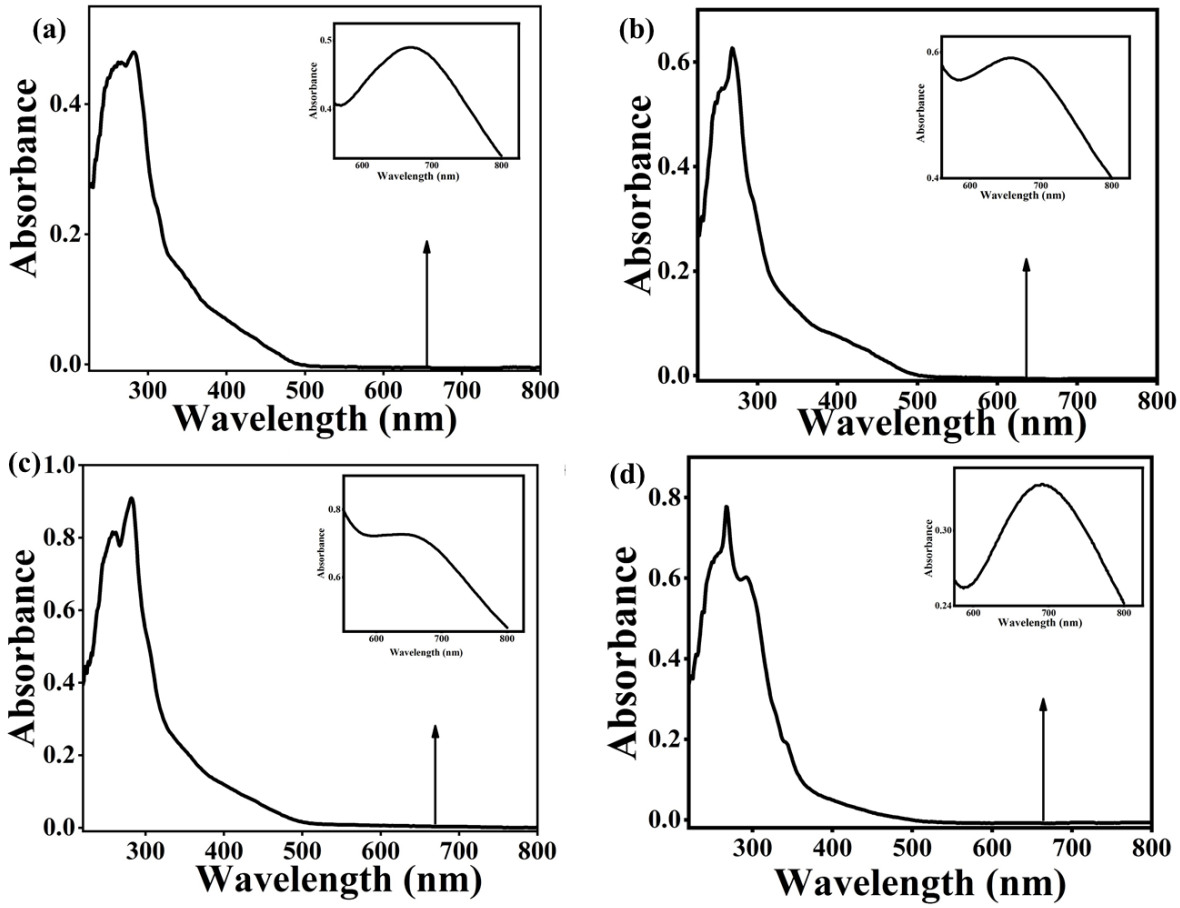

Fig. S14 (a)-(d) UV–visible absorption spectra of complexes **1-4** in DMF (1×10^{-5} M). Inset plot: Expansion of d-d band in DMF (5×10^{-3} M).

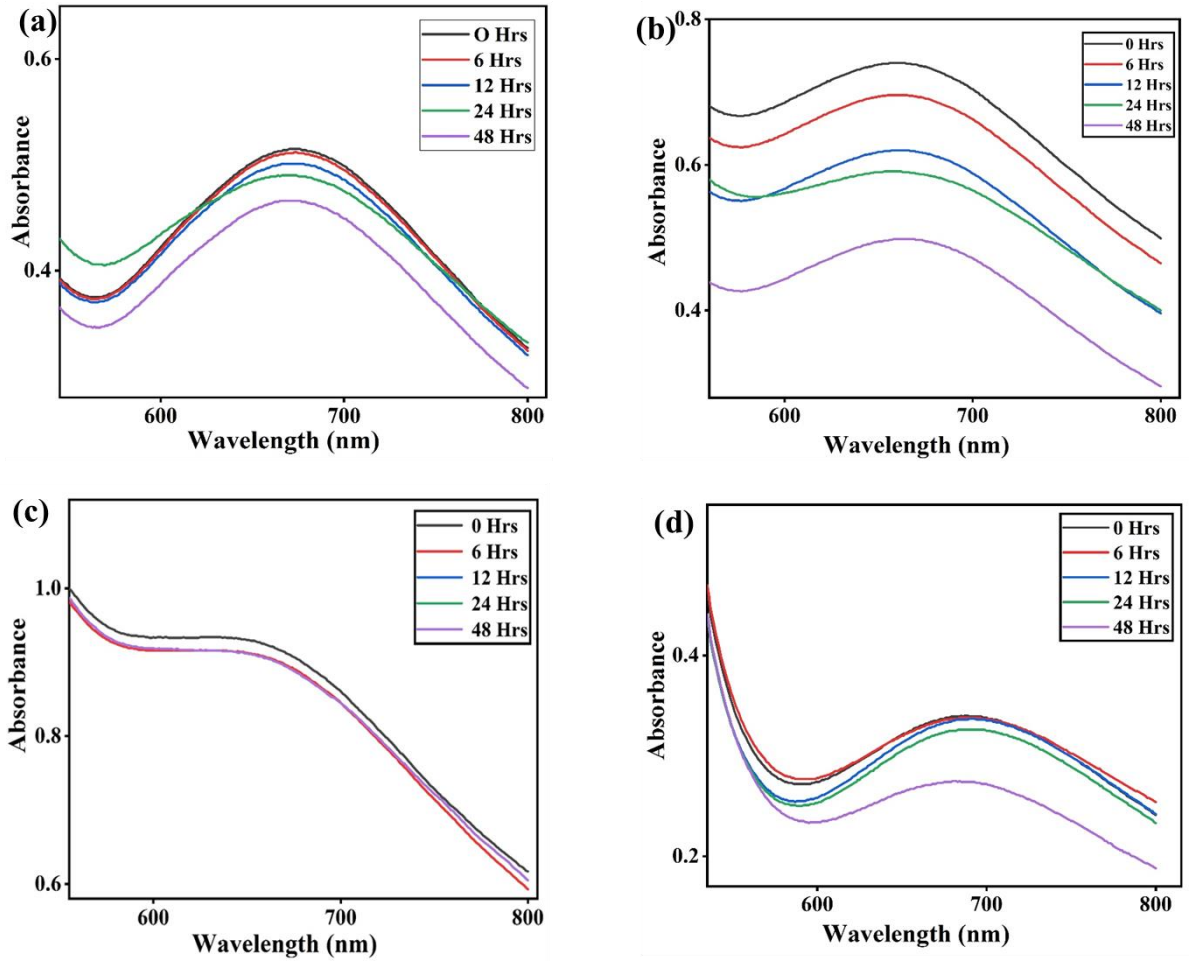

Fig. S15 (a)-(d) UV–visible absorption spectra of complexes **1-4** in DMF (5×10^{-3} M) in different time intervals.

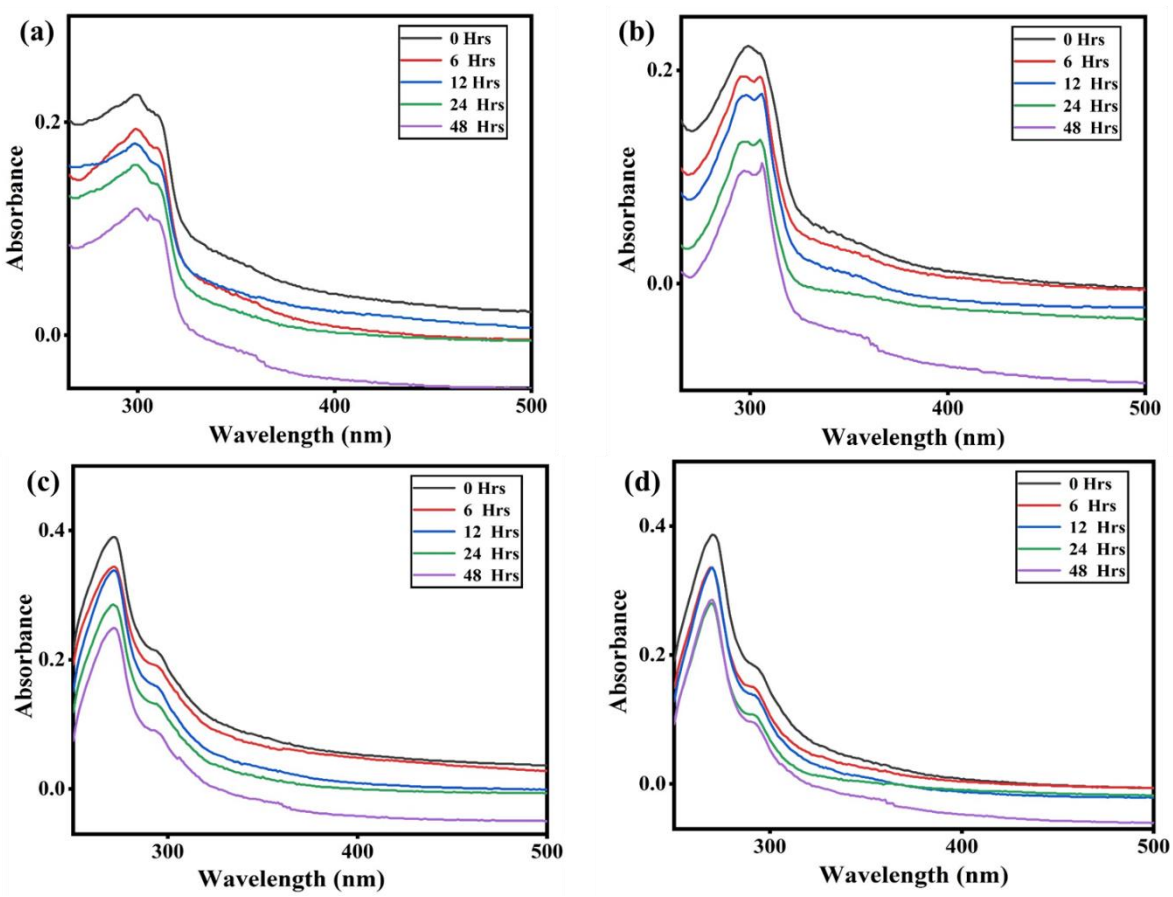
(a)
0 Hrs
6 Hrs
12 Hrs
24 Hrs
48 Hrs
Absorbance
0.2
0.0
300
400
500
Wavelength (nm)
(b)
0 Hrs
6 Hrs
12 Hrs
24 Hrs
48 Hrs
Absorbance
0.2
0.0
300
400
500
Wavelength (nm)
(c)
0 Hrs
6 Hrs
12 Hrs
24 Hrs
48 Hrs
Absorbance
0.4
0.2
0.0
300
400
500
Wavelength (nm)
(d)
0 Hrs
6 Hrs
12 Hrs
24 Hrs
48 Hrs
Absorbance
0.4
0.2
0.0
300
400
500
Wavelength (nm)

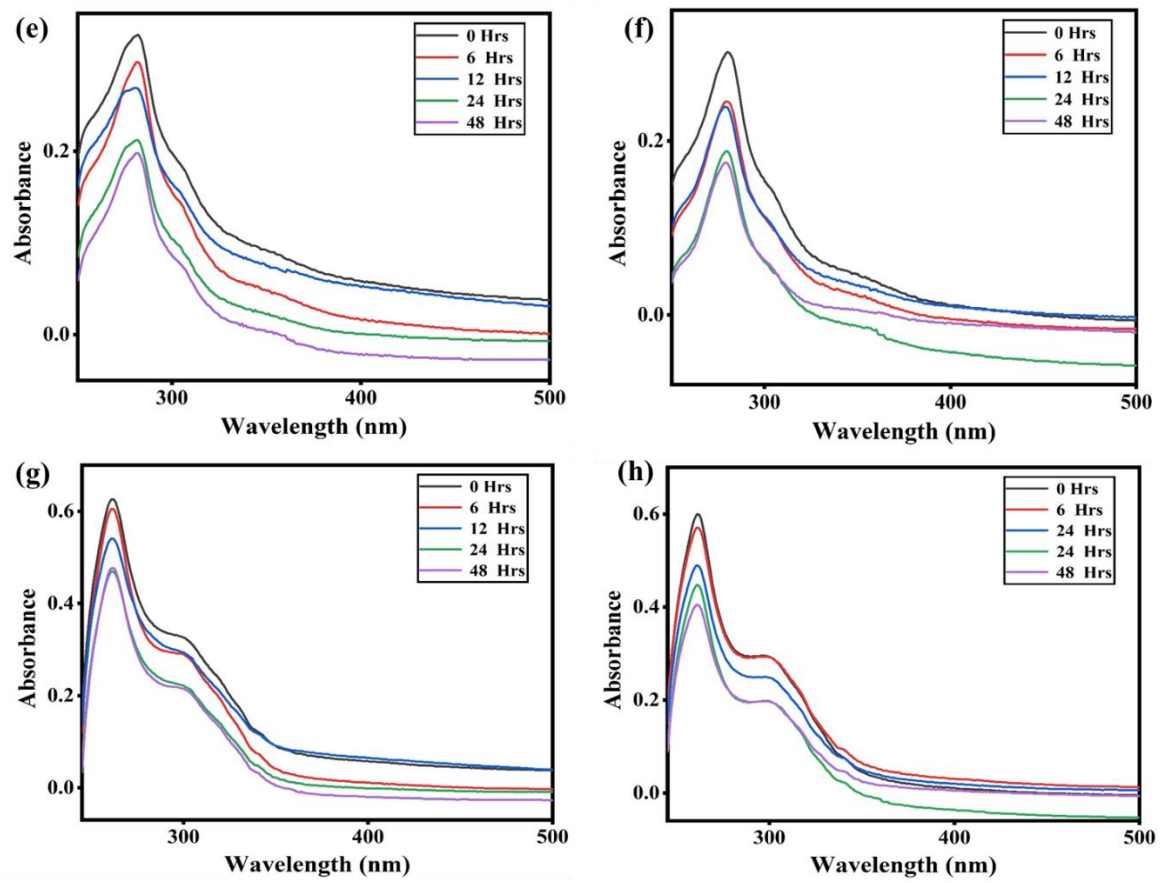

Fig. S16 (a)-(h) UV-visible absorption spectra of complexes **1-4** (1×10^{-5} M) in PBS alone (**a, c, e, g**) and with metal ions (**b, d, f, h**) Zn^{2+}, Fe^{2+}, Co^{2+}, and Ni^{2+} (1×10^{-5} M) in PBS at different time intervals.

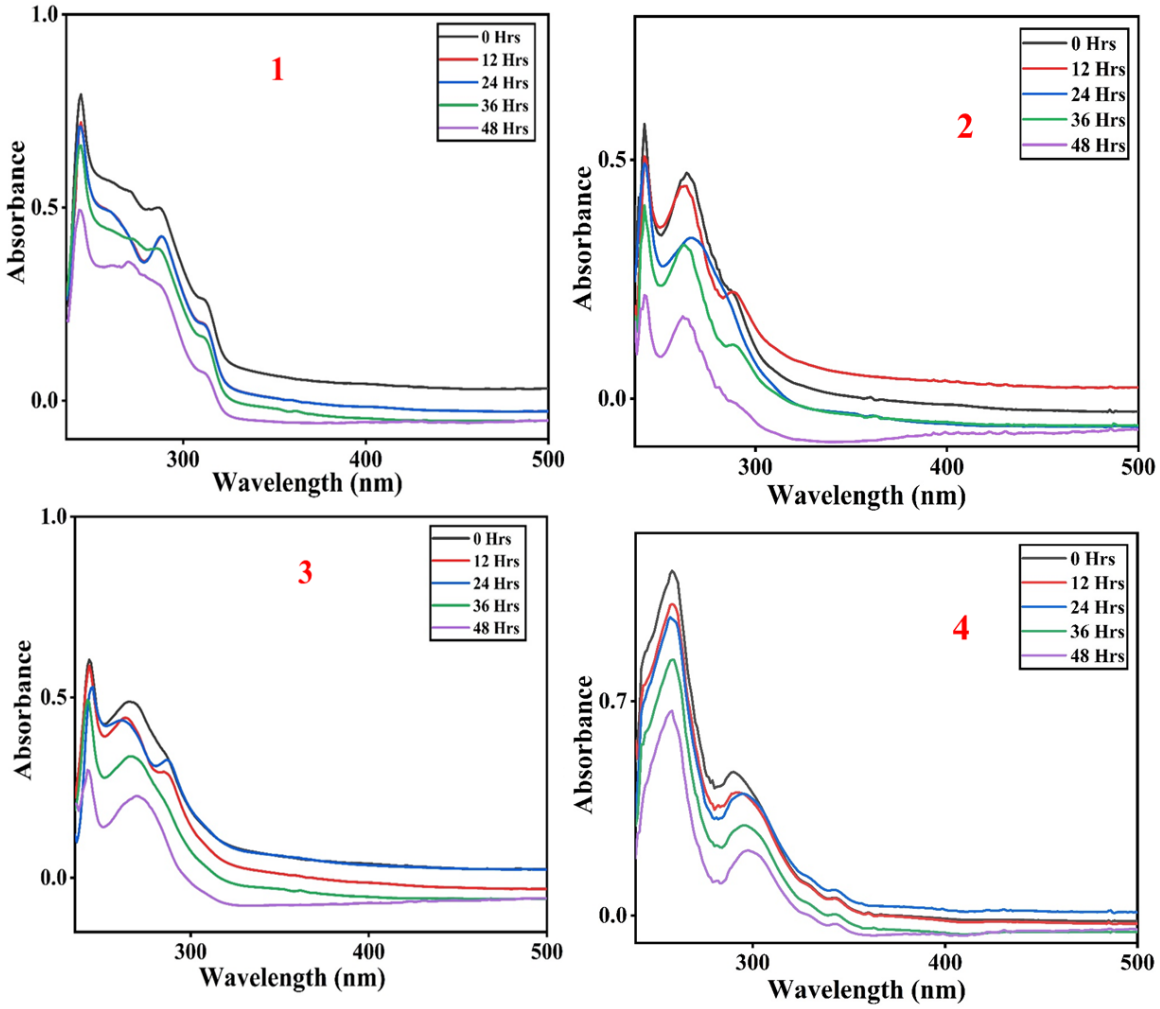

Fig. S17. UV–visible absorption spectra of complexes **1-4** in 10% Serum-PBS buffer (1×10^{-5} M) in different time intervals.

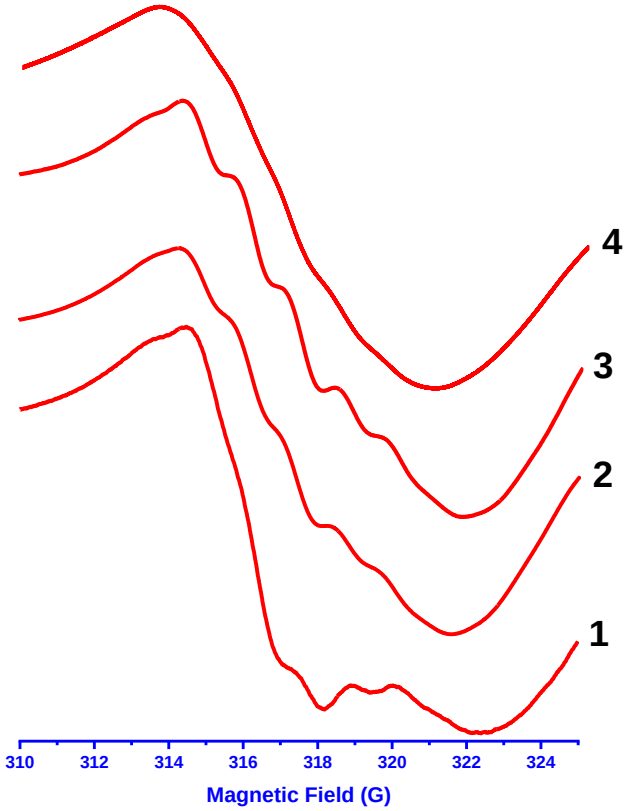

Fig. S18. *N*-super hyperfine (*N*-shf) lines of X-band EPR spectra of the complexes **1**-**4** in DMF at 77 K. Frequency 9.1-9.16 GHz.

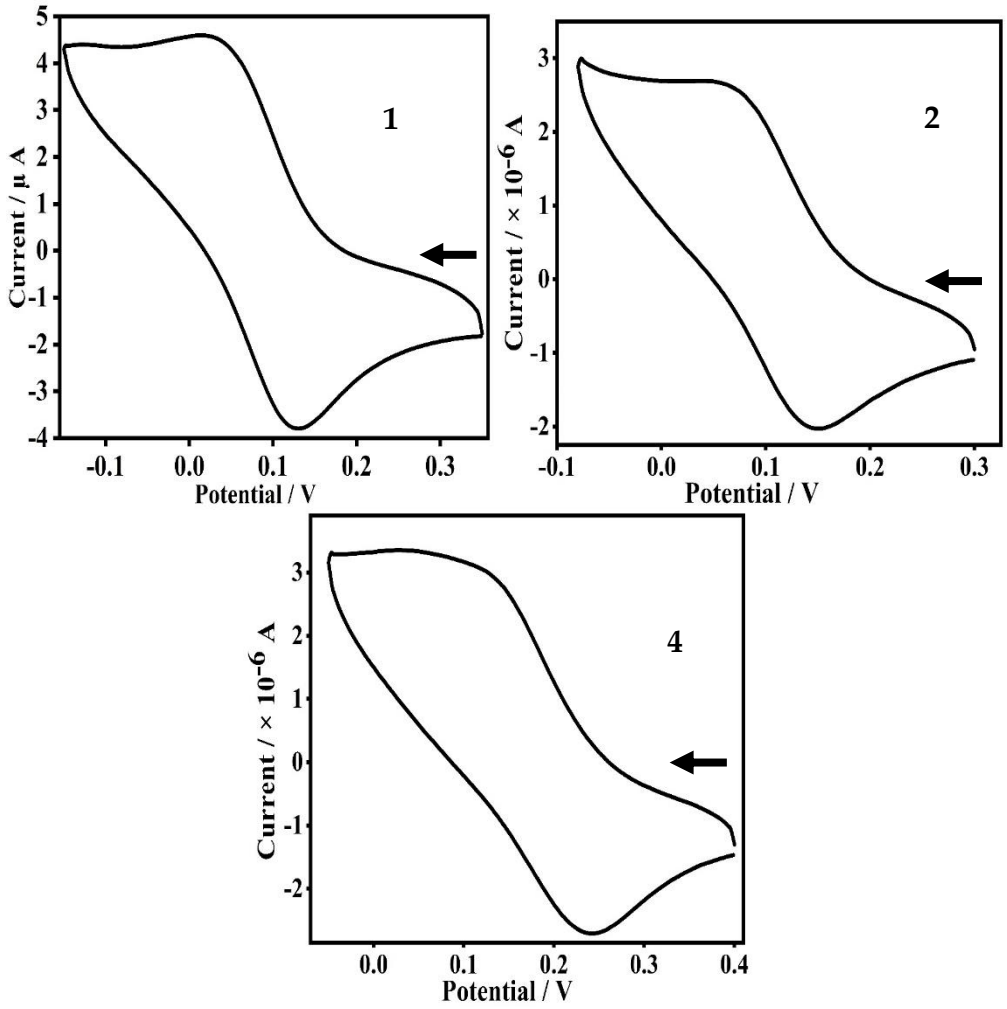

Fig. S19. Cyclic voltammogram of a 1 mmol.dm^{-3} solution of complexes **1**,**2**, and **4** in DMF in presence of 0.1 M TBAP as a supporting electrolyte and Calomel as reference electrode; scan rate 0.05 V/s, Differential pulse voltammetry, scan rate, 5 mV.s^{-1}; pulse height, 50 mV.

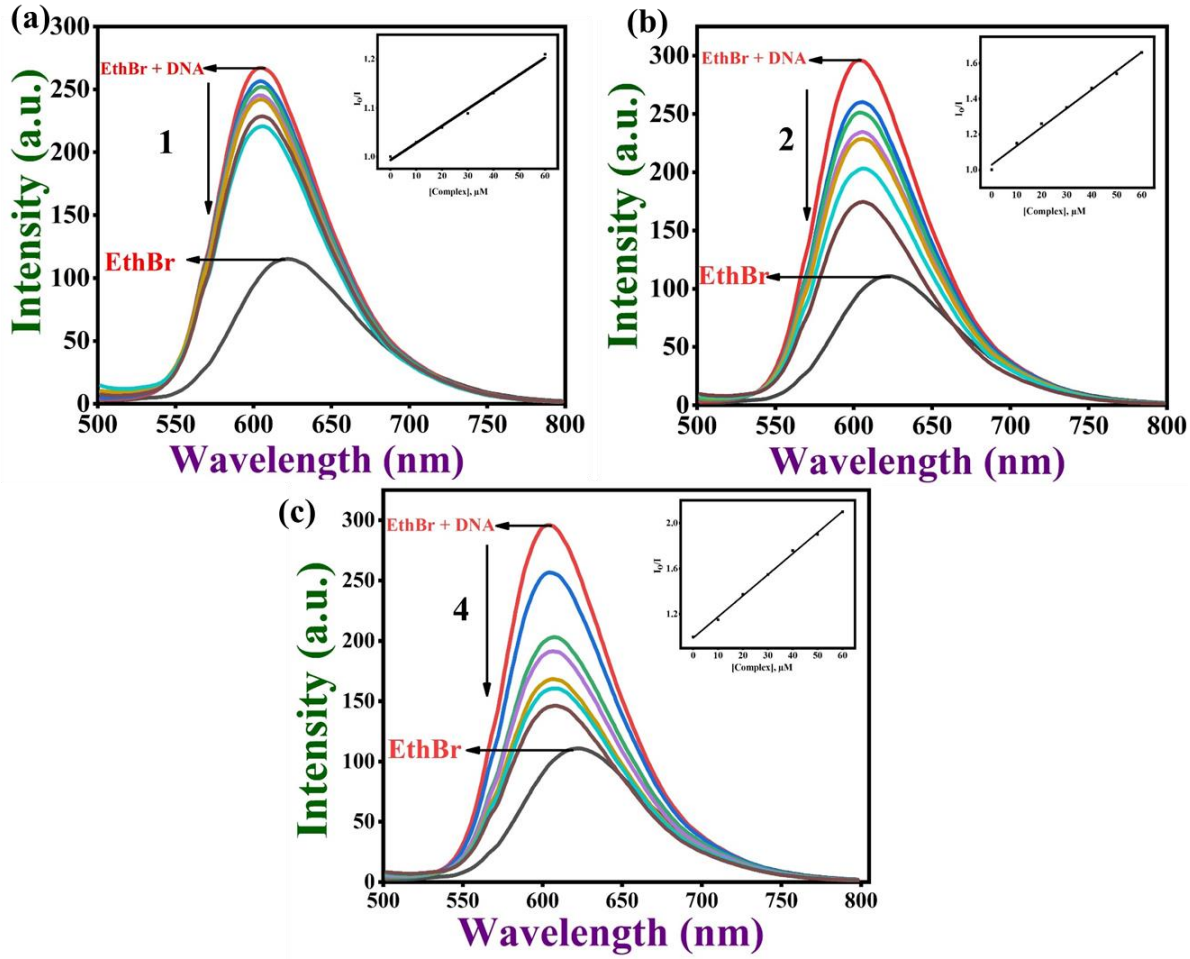

Fig. S20 (a-c) Fluorescence titration of the Cu(II) complexes **1,2** and **4** (0 - 60 μM) with DNA (125 μM). Effect of the addition of complexes **1,2** and **4** on emission intensity of CT DNA-bound EthBr. Inset: The plot of I_0/I vs [complex].

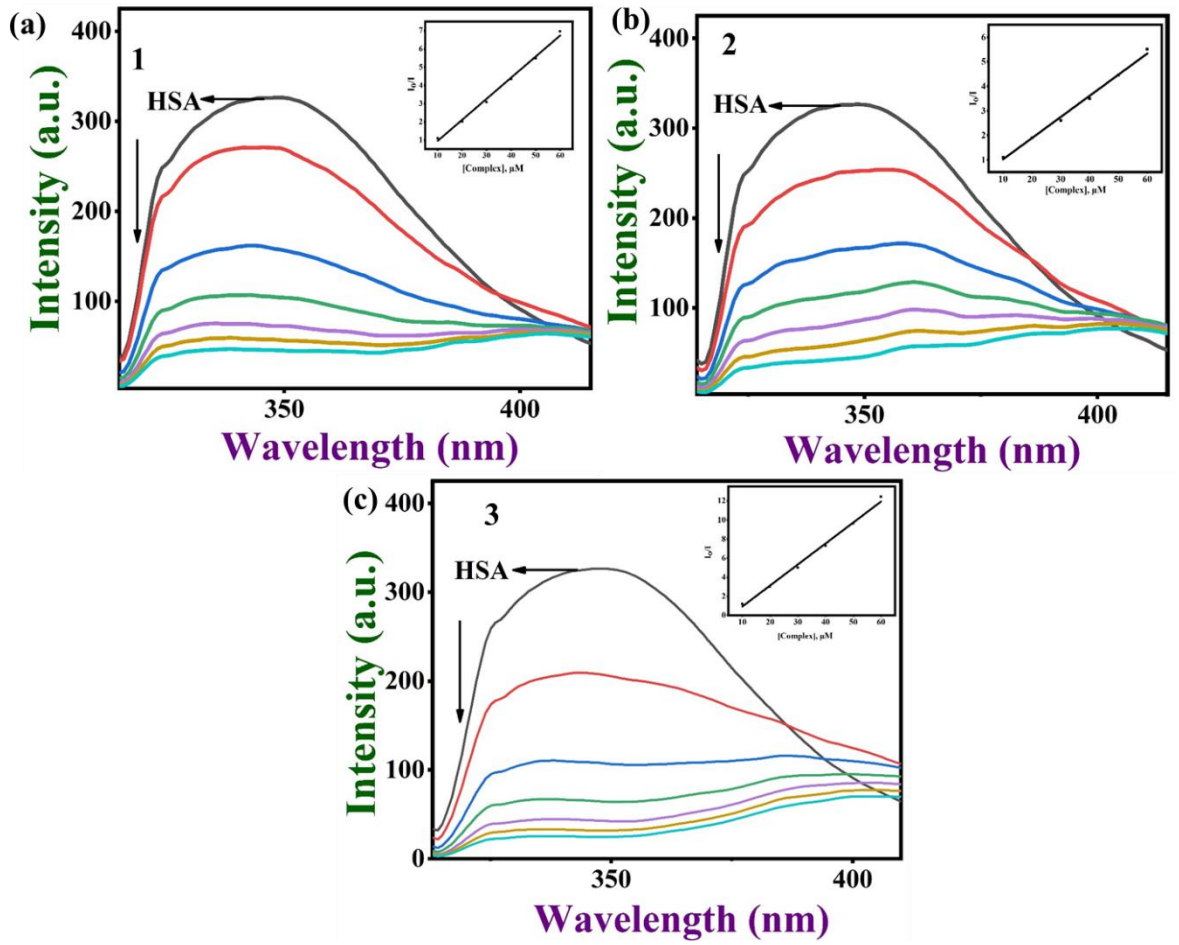

Fig. S21 (a-c). The fluorescence of HSA was gradually quenched upon adding Cu(II) complexes of **1-3** at around 347 nm at pH 7.1. Inset: The plot of I_0/I vs [complex].

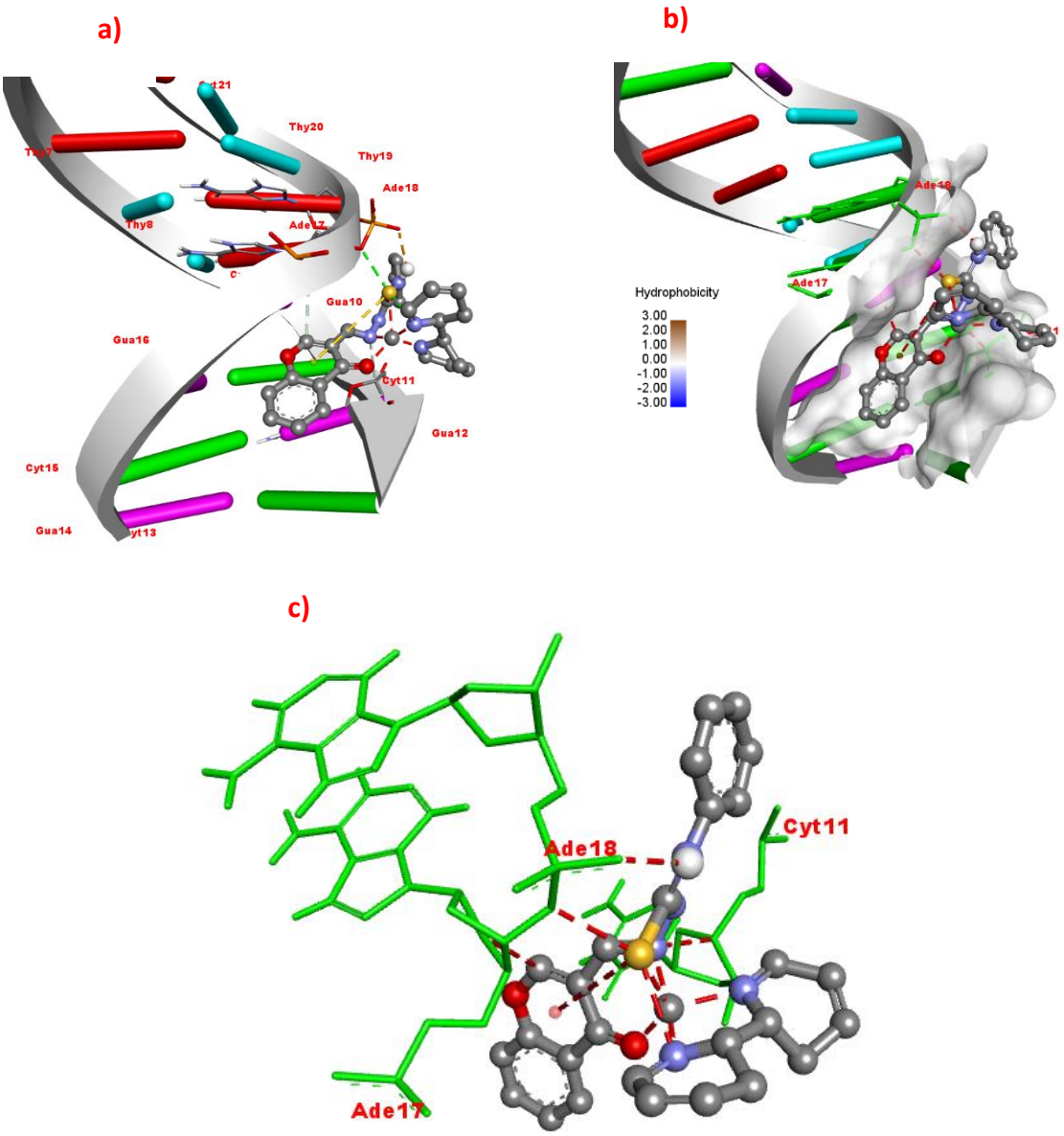

Fig. S22 Molecular docking of DNA (PDB: 1BNA) with complex **1.** (a) Full 3D-view of DNA with complex **1** in minor groove. (b) Detailed interactions of **1** with surrounding nucleobase residues. (c) 3D-view of Hydrophobic interactions with dodecamer DNA nucleobase residues.

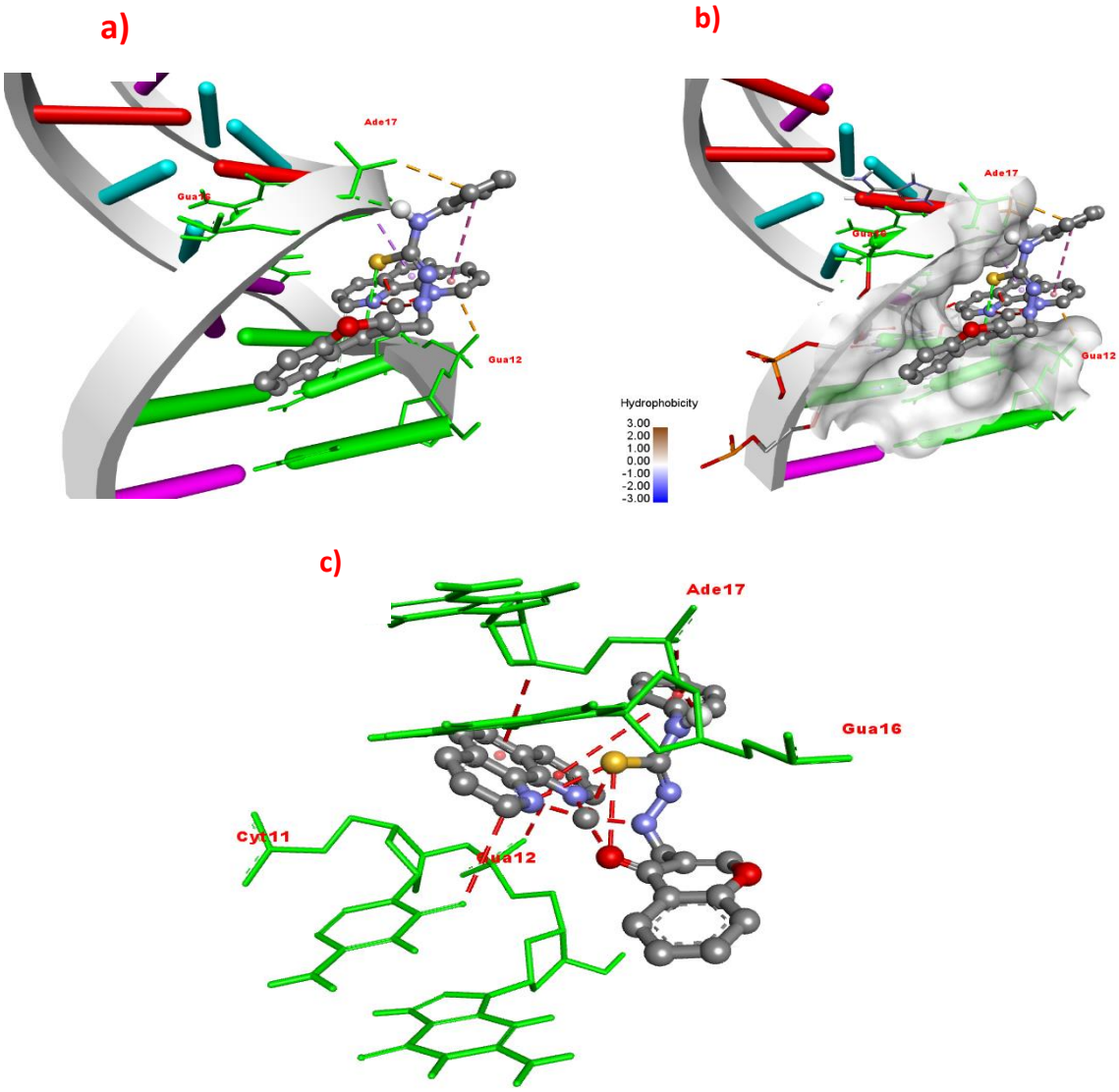

Fig. S23 Molecular docking of DNA (PDB: 1BNA) with complex **2.** (a) Full 3D-view of DNA with complex **2** in minor groove. (b) Detailed interactions of **2** with surrounding nucleobase residues. (c) 3D-view of Hydrophobic interactions with dodecamer DNA nucleobase residues.

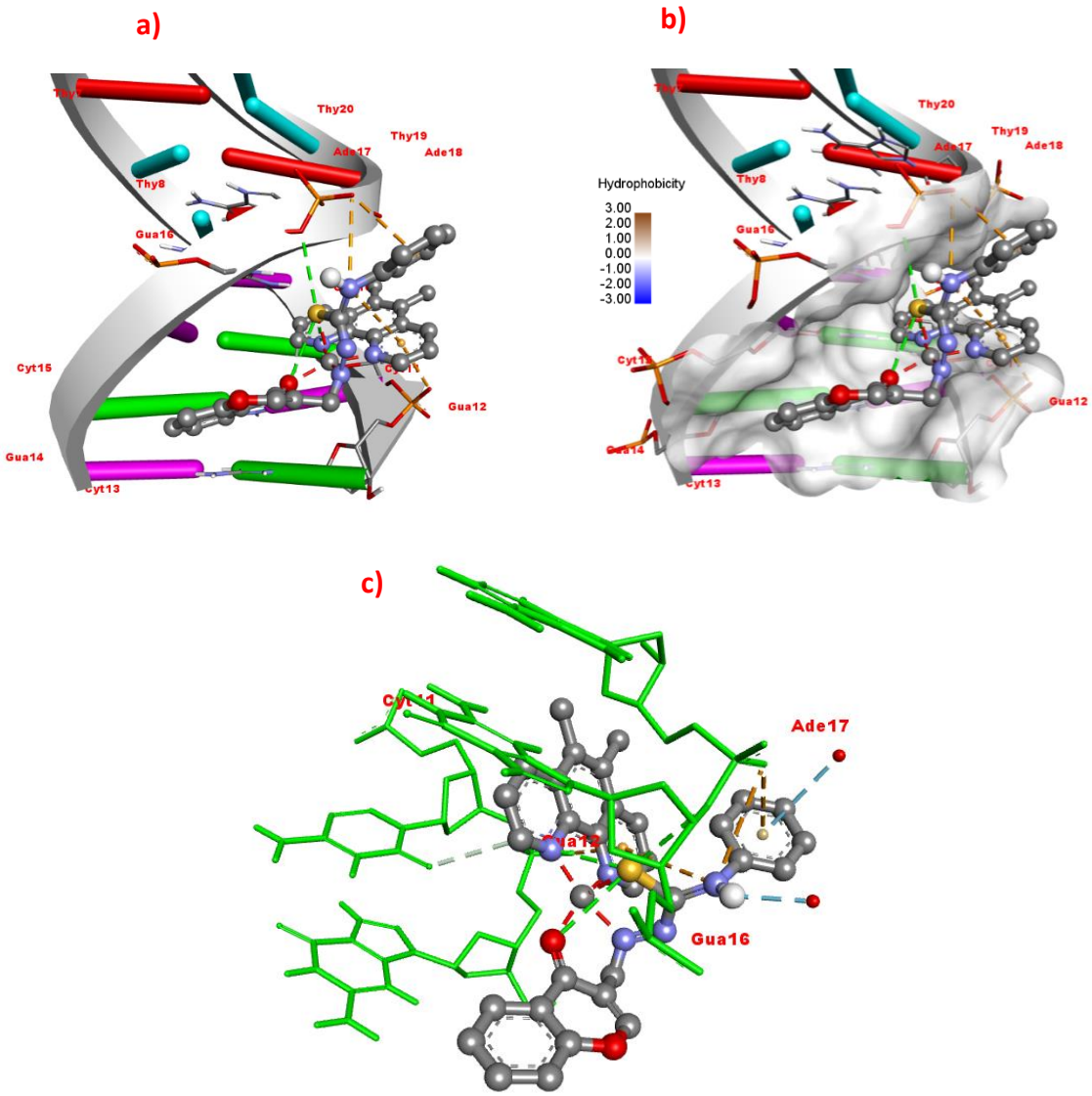

Fig. S24 Molecular docking of DNA (PDB: 1BNA) with complex **3.** (a) Full 3D-view of DNA with complex **3** in minor groove. (b) Detailed interactions of **3** with surrounding nucleobase residues. (c) 3D-view of Hydrophobic interactions with dodecamer DNA nucleobase residues.

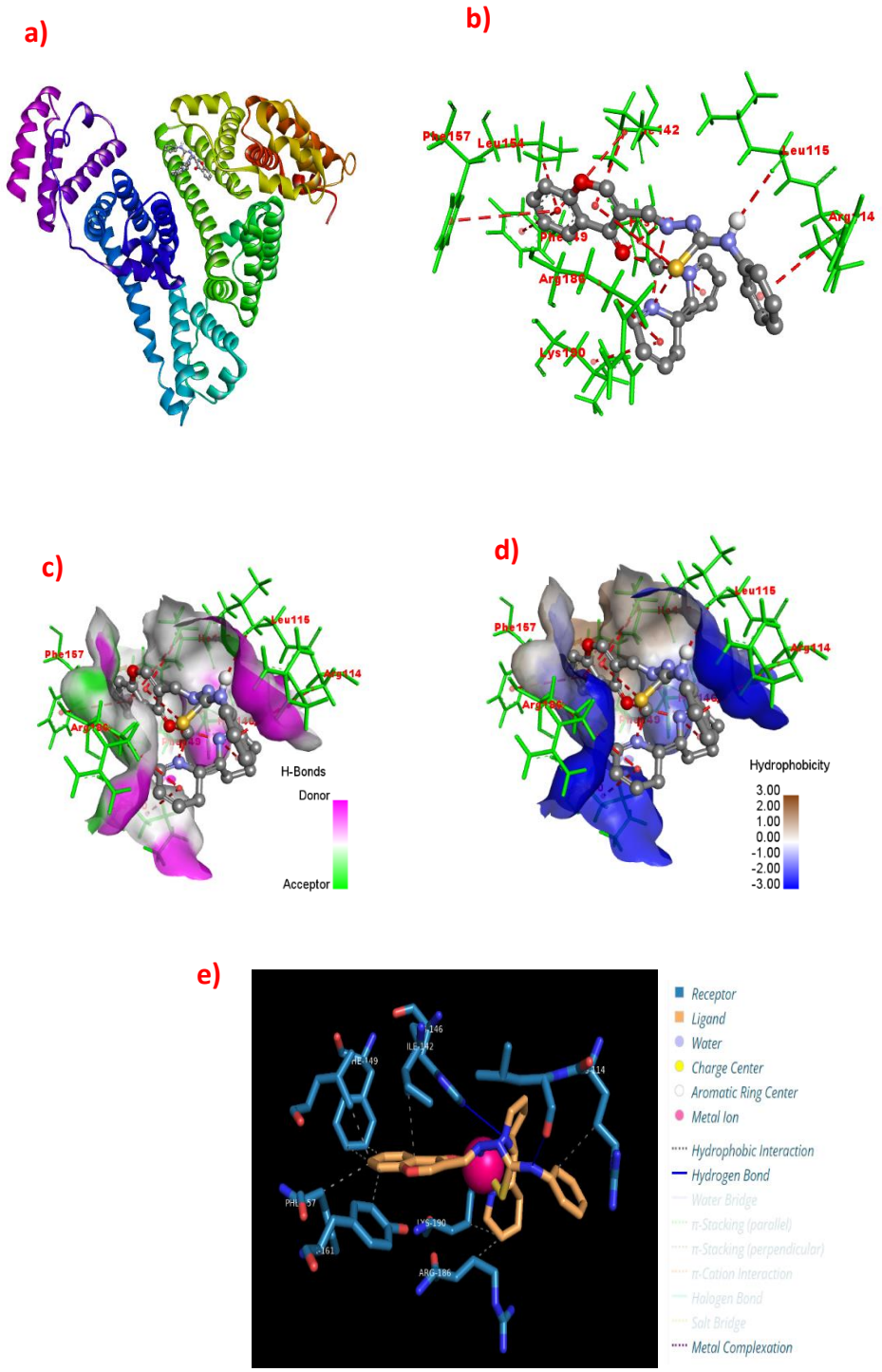

Fig. S25 Molecular docking of HSA (PDB: 8H0O) with complex **1.** (a) Full view of HSA with color-coded subdomains showing the binding site of **1** in HSA. (b) Detailed interactions of **1** with surrounding amino acid residues. (c) 3D-view of Hydrogen bond interactions. (d) 3D-view of Hydrophobic interactions with amino acid residues. (e) Detailed interaction of **1** with surrounding amino acid residues.

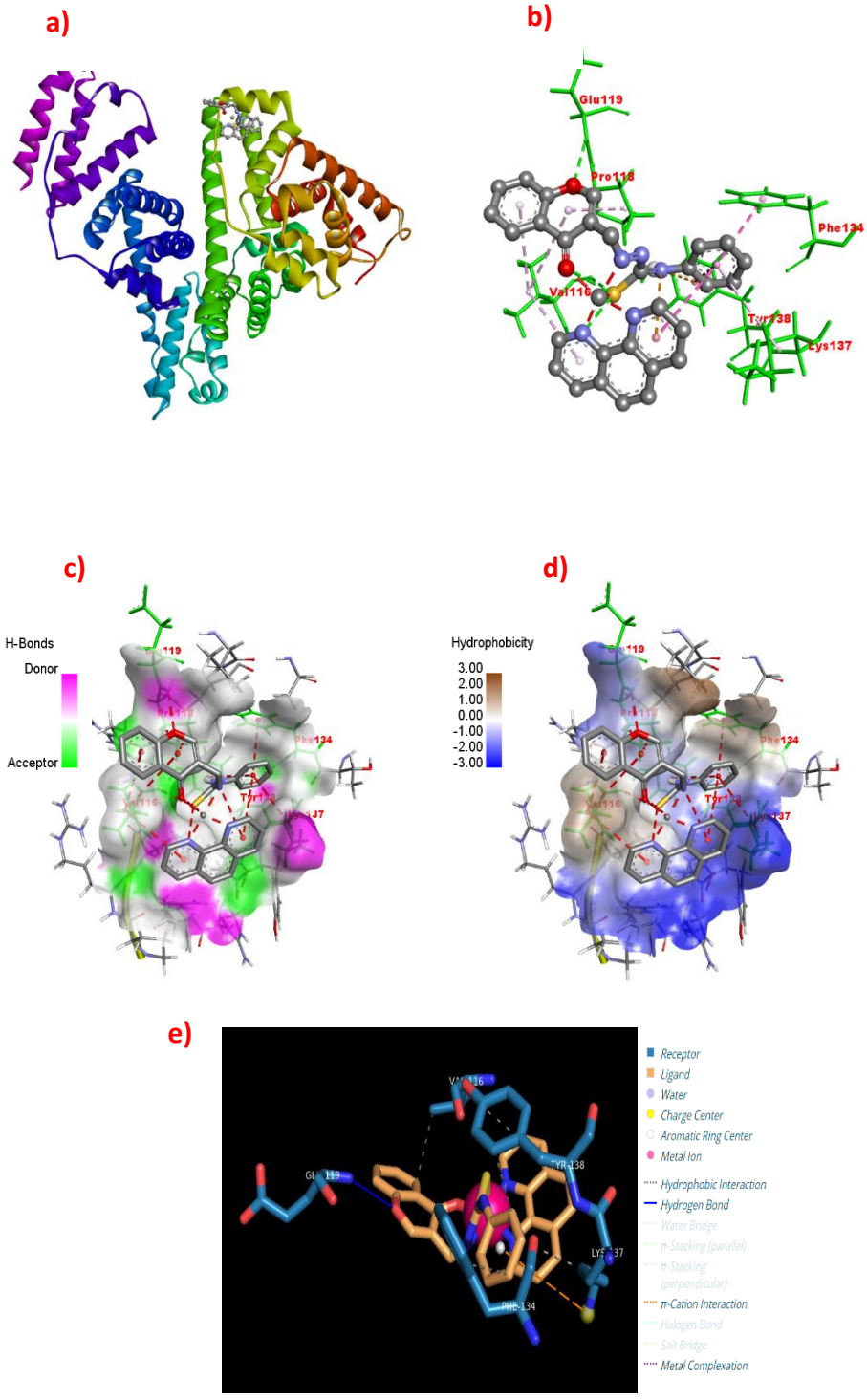

Fig. S26 Molecular docking of HSA (PDB: 8H0O) with complex **2.** (a) Full view of HSA with color-coded subdomains showing the binding site of **2** in HSA. (b) Detailed interactions of **2** with surrounding amino acid residues. (c) 3D-view of Hydrogen bond interactions. (d) 3D-view of Hydrophobic interactions with amino acid residues. (e) Detailed interaction of **2** with surrounding amino acid residues.

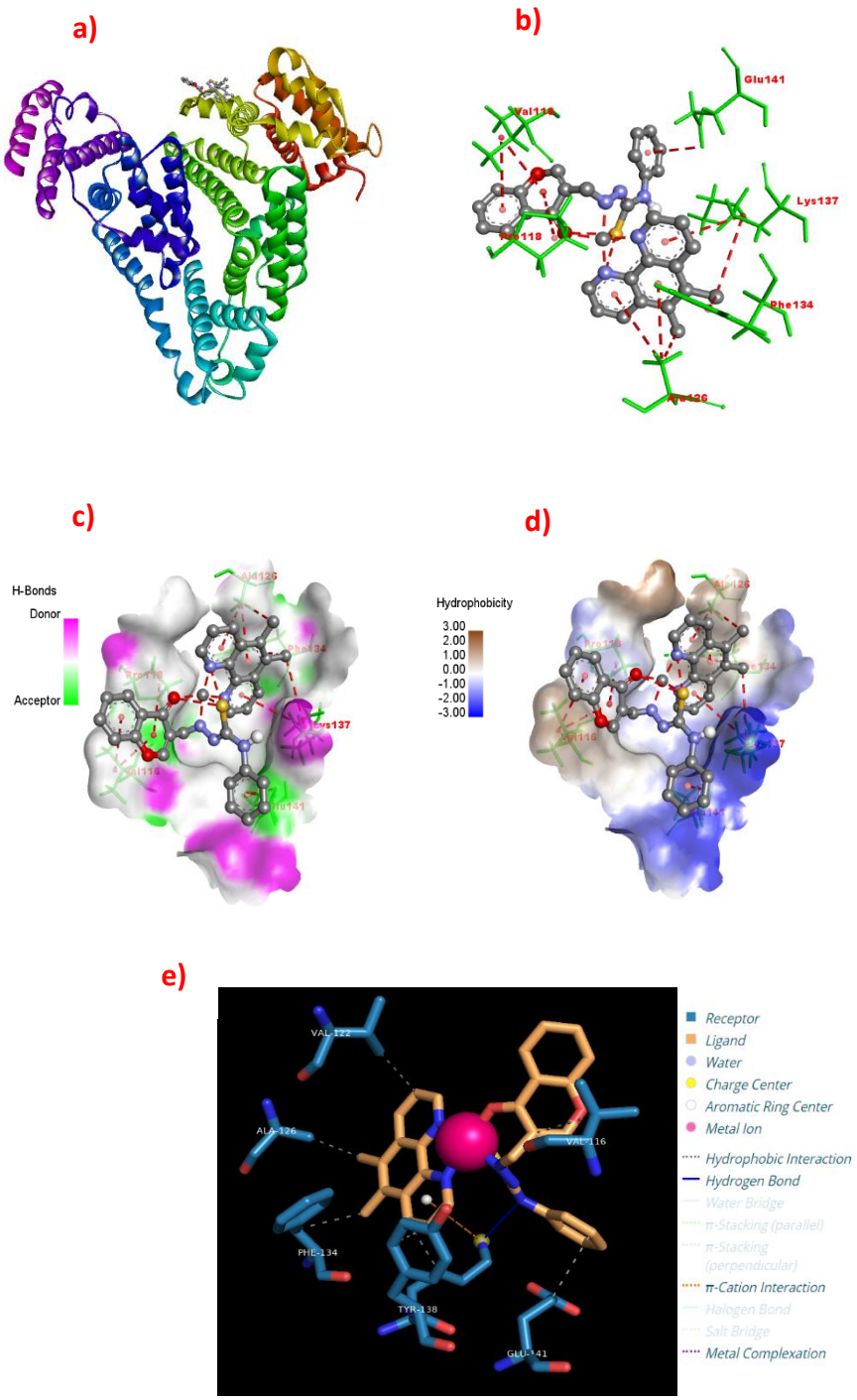

Fig. S27 Molecular docking of HSA (PDB: 8H0O) with complex **3.** (a) Full view of HSA with color-coded subdomains showing the binding site of **3** in HSA. (b) Detailed interactions of **3** with surrounding amino acid residues. (c) 3D-view of Hydrogen bond interactions. (d) 3D-view of Hydrophobic interactions with amino acid residues. (e) Detailed interaction of **3** with surrounding amino acid residues.

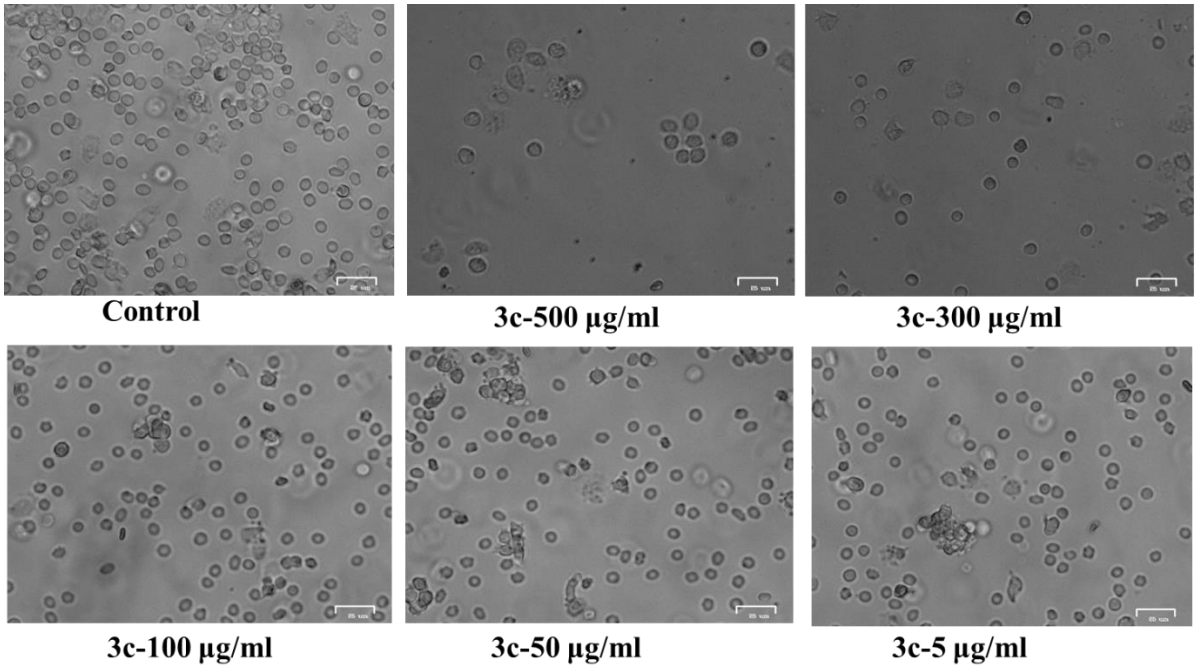

Fig. S28 Images of control cells and Complex **3** with treated cells

Table S1 Molar conductance values for copper(II) complexes **1**-**4** in DMF

Complex	Molar Conductance Λ_M /Ω^{-1} cm^2 mol^{-1}
1	55
2	59
3	50
4	55

Table S2. Computed bond lengths and HOMO and LUMO energies and energy gap of complexes $[Cu(L)(diimine)]^{1+}$ (**1–4**).

Bonds	Bond Lengths (Å)			
	1	**2**	**3**	**4**
Cu–O1	2.077	2.062	2.068	2.055
Cu–N1	2.008	2.010	2.009	2.008
Cu–S1	2.408	2.401	2.403	2.397
Cu–N2	2.007	2.017	2.013	2.022
Cu–N3	2.184	2.232	2.215	2.232

Table S3 Computed bond angles [°] of complexes $[Cu(L)(diimine)]^{1+}$ (**1–4**).

Bond angles/°	**1**	**2**	**3**	**4**
O1–Cu–N1	90.080	90.462	90.429	90.694
O1–Cu–S1	153.337	156.724	156.767	157.767
O1–Cu–N2	90.022	90.231	90.006	90.017
O1–Cu–N3	94.847	93.377	93.114	93.638
N1–Cu–S1	84.739	84.902	84.858	84.988
N1–Cu–N2	176.372	175.739	175.161	175.572
N1–Cu–N3	103.955	103.897	104.731	104.569
S1–Cu–N2	93.562	92.820	92.864	92.718
S1–Cu–N3	111.792	109.883	110.094	108.564
N2–Cu–N3	79.650	80.258	80.056	79.744
Trigonality index, τ	0.38	0.32	0.31	0.30

Table S4. Computed HOMO and LUMO energies and energy gap of complexes $[Cu(L)(diimine)]^{1+}$ (**1–4**).

Complex / Energy (eV)	**1**	**2**	**3**	**4**
Optimized energy	-4.547×10^4	-4.755×10^4	-4.969×10^4	-5.260×10^4
HOMO	-6.073	-6.074	-6.066	-6.084
LUMO	-2.920	-2.932	-2.922	-2.952
Energy Gap	3.153	3.142	3.144	3.132

Table S5 UV-visible spectral data of complexes **1-4** in the absence and presence of metal ions in PBS at various time intervals.

S.No	Complex	Condition	λ_{abs}	Wavelength (nm)					Condition	λ_{abs}	Wavelength (nm)				
				0 Hr	6 Hr	12 Hr	24 Hr	48 Hr			0 Hr	6 Hr	12 Hr	24 Hr	48 Hr
1.	**1**	PBS	Wavelength 1	299	299	299	298	299	In the presence of metal ions (Zn^{2+}, Fe^{2+}, Co^{2+}, Ni^{2+}) in PBS	Wavelength 1	299	298	298	298	297
2.	**2**	PBS	Wavelength 1	272	272	272	271	271	In the presence of metal ions (Zn^{2+}, Fe^{2+}, Co^{2+}, Ni^{2+}) in PBS	Wavelength 1	270	269	270	270	269
			Wavelength 2	295	295	295	295	295		Wavelength 2	294	294	294	294	294
3.	**3**	PBS	Wavelength 1	282	282	281	281	281	In the presence of metal ions (Zn^{2+}, Fe^{2+}, Co^{2+}, Ni^{2+}) in PBS	Wavelength 1	280	279	279	280	279
			Wavelength 2	307	307	307	307	307		Wavelength 2	306	305	306	306	305
4.	**4**	PBS	Wavelength 1	262	262	261	261	262	In the presence of metal ions (Zn^{2+}, Fe^{2+}, Co^{2+}, Ni^{2+}) in PBS	Wavelength 1	261	261	261	261	261
			Wavelength 2	302	302	301	302	302		Wavelength 2	302	302	301	302	302

Table S6. Cleavage data of SC pUC19 DNA by complexes **1-4** in the absence of any reducing agent for an incubation time of 4 h.

Lane No.	Reaction Condition	Form %	
		SC	NC
1	DNA (40 μM)	91	09
2	DNA (40 μM) + **1** (100 μM)	90	10
3	DNA (40 μM) + **2** (100 μM)	81	19
4	DNA (40 μM) + **3** (100 μM)	48	52
5	DNA (40 μM) + **4** (100 μM)	84	16
6	DNA (40 μM) + **$[Cu(dpq)_2]^{2+}$** (100 μM)	02	98

Table S7. Data of SC pUC19 DNA cleavage by complexes **1c-4c** in the presence of the reductant ascorbic acid for an incubation time of 30 min.

Lane No.	Reaction Condition	Form %	
		SC	NC
1	DNA (40 μM)	88	12
2	DNA (40 μM) + H_2A	84	16
3	DNA (40 μM) + H_2A + **1** (100 μM)	80	20
4	DNA (40 μM) + H_2A + **2** (100 μM)	00	100
5	DNA (40 μM) + H_2A + **3** (100 μM)	00	100
6	DNA (40 μM) + H_2A + **4** (100 μM)	40	60
7	DNA (40 μM) + H_2A + **$[Cu(dpq)_2]^{2+}$** (100 μM)	06	94

Table S8. Data of SC pUC19 DNA cleavage by complex **3c** in the presence of the reductant ascorbic acid and various radical scavengers for an incubation time of 30 minutes

		Form %	
Lane No.	**Reaction Condition**	**SC**	**NC**
1	DNA (40 µM)	90	10
2	DNA (40 µM)+ H_2A + **3** (100µM)	00	100
3	DNA (40 µM) + H_2A + **3** (100µM) + 10% DMSO	00	100
4	DNA (40 µM) + H_2A +**3** (100µM) + 50µM NaN_3	00	100
5	DNA (40 µM) + H_2A +**3** (100µM) + Catalase (0.1Unit)	86	14
6	DNA (40 µM) + H_2A +**3** (100µM) + SOD (1Unit)	00	100
7	DNA (40 µM) + H_2A +**3** (100µM) + N_2	00	100

References

1 A. Kleineweischede and J. Mattay, *European J. Org. Chem.*, 2006, 947–957.

2 R. Loganathan, S. Ramakrishnan, E. Suresh, A. Riyasdeen, M. A. Akbarsha and M. Palaniandavar, *Inorg. Chem.*, 2012, **51**, 5512–5532.

3 S. Ramakrishnan, V. Rajendiran, M. Palaniandavar, V. S. Periasamy, B. S. Srinag, H. Krishnamurthy and M. A. Akbarsha, *Inorg. Chem.*, 2009, **48**, 1309–1322.

4 S. Karpagam, R. Kartikeyan, P. Paravai Nachiyar, M. Velusamy, M. Kannan, M. Krishnan, U. Chitgupi, J. F. Lovell, M. Abdulkader Akbarsha and V. Rajendiran, *J. Coord. Chem.*, 2019, **72**, 3102–3127.

5 T. Khamrang, R. Kartikeyan, M. Velusamy, V. Rajendiran, R. Dhivya, B. Perumalsamy, M. A. Akbarsha and M. Palaniandavar, *RSC Adv.*, 2016, **6**, 114143–114158.

6 S. Kasibhatla, G. P. Amarante-Mendes, D. Finucane, T. Brunner, E. Bossy-Wetzel and D. R. Green, *Csh Protoc*.

7 C. Zhang, M.-L. Maddelein, R. W.-Y. Sun, H. Gornitzka, O. Cuvillier and C. Hemmert, *Eur. J. Med. Chem.*, 2018, **157**, 320–332.

8 S. Karpagam, A. Mamindla, V. Kumar, R. Sankaran, V. Subbarayan, A. Abdullah, M. Abdulkader and V. Rajendiran, *Inorg. Chim. Acta*, 2022, **531**, 120729.

9 K. Radhakrishnan, T. Khamrang, K. Sambantham, V. K. Sali, U. Chitgupi, J. F. Lovell, A. A. Mohammad and R. Venugopal, *Polyhedron*, 2021, **194**, 114886.

10 B. Selvakumar, V. Rajendiran, P. Uma Maheswari, H. Stoeckli-Evans and M. Palaniandavar, *J. Inorg. Biochem.*, 2006, **100**, 316–330.

11 Y.-Q. Wang, H.-M. Zhang, G.-C. Zhang, W.-H. Tao and S.-H. Tang, *J. Lumin.*, 2007, **126**, 211–218.

12 U. K. Laemmli, *Nature*, 1970, **227**, 680–685.

13 O. H. Lowry, N. J. Rosebrough, A. L. Farr and R. J. Randall, *J. Biol. Chem.*, 1951, **193**, 265–275.

14 M. T. Carter, M. Rodriguez and A. J. Bard, *J. Am. Chem. Soc.*, 1989, **111**, 8901–8911.

15 J. Bernadou, G. Pratviel, F. Bennis, M. Girardet and B. Meunier, *Biochemistry*, 1989, **28**, 7268–7275.

16 V. K. Vishvakarma, K. Kumari, R. Patel, V. S. Dixit, P. Singh, G. K. Mehrotra, R. Chandra and A. K. Chakrawarty, *Spectrochim. Acta - Part A Mol. Biomol. Spectrosc.*, 2015, **143**, 319–323.